1-1-2006

The Fourier convolution-deconvolution method: its limitation and application

Nicole Teresa Gugliotta
Iowa State University

The Fourier convolution-deconvolution method: Its limitation and application

by

Nicole Teresa Gugliotta

A thesis submitted to the graduate faculty

in partial fulfillment of the requirements for the degree of

MASTER OF SCIENCE

Major: Chemistry

Program of Study Committee:
Yeon-Kyun Shin, Co-major Professor
Thomas Greenbowe, Co-major Professor
Klaus Schmidt-Rohr

Iowa State University

Ames, Iowa

2006

Graduate College
Iowa State University

This is to certify that the master's thesis of

Nicole Teresa Gugliotta

has met the thesis requirements of Iowa State University

Signatures have been redacted for privacy

TABLE OF CONTENTS

CHAPTER 1: GENERAL INTRODUCTION 1

EPR Theory 1

SNARE Proteins and Membrane Fusion 3

References 4

CHAPTER 2: EXTENDING THE LIMITS OF THE CWEPR SPECTROSCOPIC RULER 11

Introduction 11

The Fourier Convolution-Deconvolution Method 11

Methods 16

Results and Discussion 21

Conclusions 23

References 23

CHAPTER 3: DETERMINING PROTEIN CONFORMATION USING THE EPR SPECTROSCOPIC RULER 37

Introduction 37

Methods 39

Results and Discussion 44

Conclusions 45

References 45

CHAPTER 4: GENERAL CONCLUSIONS 50

Conclusions 50

References 51

ACKNOWLEDGEMENTS 53

CHAPTER 1: GENERAL INTRODUCTION

EPR Theory

The atom is composed of a nucleus, containing protons and neutrons, as well as electrons found within a certain probability of the nucleus. NMR (nuclear magnetic resonance) instrumentation provides scientists with the ability to determine the local structure of biomolecules based on the phenomenon of quantized nuclear magnetic moments. Unlike NMR, the use of EPR/ESR (electron paramagnetic resonance/electron spin resonance) instrumentation is not limited to protein or sample size (Biswas *et al.*, 2001). Therefore more proteins can be studied with EPR than with NMR. EPR, on the other hand, comes as a result of the quantization of electron magnetic moments. The magnetic moment, μ, is directly related to the spin state of the electron,

$$\mu = -g\beta S.$$

S represents the spin state of the electron while β and g are constants that represent the Bohr magneton and *g*-factor, respectively. The Bohr magneton is a constant that reflects the magnetic moment of the electron with respect to its mass. The *g*-factor is dependent upon the orbital motion within the atom and therefore reflects the local environment of the electron. It is positioned in the center of the middle hyperfine line of a first-derivative mode spectrum. The *g*-factor for a free electron is 2.0023 and the g-factor for a nitroxide spin label varies between 2.0020 and 2.0090. *g*-factors that vary most from that of a free electron are the unpaired electrons of transition metals. The negative sign in the equation above indicates the magnetic moment is in the opposite direction of the spin (Knowles *et al.*, 1976).

In solution, with no external stimuli, the spin states of all unpaired electrons are equal in energy. However, in the presence of a magnetic field, some spins will align with the magnetic field while other spins orient themselves anti-parallel to the magnetic field. The spin-state that is aligned with the magnetic field (spin +½) is higher in energy than the spin state aligned anti-parallel to the field (spin -½) (Knowles *et al.*, 1976).

When the microwave frequency matches that of the magnetic cavity, the radiation is absorbed by the lower energy spin, exciting it to the higher energy state. This is referred to as resonance. The energy of the unpaired electron in a magnetic field, with a radiation source applied to it, is

$$E = h\upsilon = \pm\tfrac{1}{2}g\beta B,$$

where B represents the strength of the magnetic field, υ represents the frequency of the electromagnetic radiation applied, and h represents Planck's constant, as seen in Figure 1.1 (Knowles *et al.*, 1976).

In the case of site directed spin labeling (SDSL), a nitroxide spin label undergoes a chemical reaction with a particular residue within the amino acid sequence of a protein to create a covalent bond. SDSL labels are highly stable and give well resolved signals (Biswas *et al.*, 2001). This technique has made it possible to determine the local environment of a protein that does not contain any naturally occuring unpaired electrons. The most common spin label used in biophysical research is a nitroxide spin label. This type of spin label contains an unpaired electron in the p-orbital of a nitrogen atom covalently bonded to an oxygen atom. The free electron interacts with the nuclear spin of the nitrogen, which in turn interacts with the magnetic field, yielding a spectrum of three hyperfine lines reflecting the spin states of nitrogen: -1, 0, 1, as shown in Figure 1.2 (Biswas *et al.*, 2001; Knowles *et al.*,

1976). One example of a nitroxide spin label is methanethiosulfonate spin label (MTSL). MTSL produces a disulfide bond by reacting with the sulfur of a cysteine residue (Figure 1.3). Site directed spin labeling requires the amino acid of interest to be mutated to cysteine so that it may be later spin labeled. A naturally occurring cysteine would be mutated to an alanine or a serine in order to avoid spin labeling at an undesired position in the protein. The advantages of using MTSL instead of other spin labels include (1) cysteines are rare in the non-disulfide bonded form, (2) its small size, (3) the flexibility of the side chain, and (4) the fast reaction it has with cysteines under mild conditions in buffer (Biswas *et al.*, 2001; Hustedt & Beth, 1999).

SNARE Proteins and Membrane Fusion

Membrane fusion is a common occurrence throughout the biological world. This phenomenon is vital to the process of exocytosis and the transport of chemicals out of the cell. The fusion of two opposing membranes is an energetically costly process. To drive membrane fusion to completion, conserved proteins integrated into both the vesicle and target membranes (v- and t-SNAREs) come together to form a parallel four-helix bundle, which assists in the fusion process, as seen in Figure 1.4 (Poirier *et al.*, 1998). These proteins are called SNARE proteins (soluble N-ethylmalemide associated receptor proteins). NSF and SNAP are post-fusion accessory proteins used for disassembly of the SNARE complex to be recycled for further membrane fusion (for review, see Bennett & Scheller, 1994).

SNARE proteins are necessary for membrane fusion in several instances. For example, synaptic vesicles containing neurotransmitters must fuse with the plasma membrane of a neuron for the release of the neurotransmitters into the synapse cleft from the

pre-synaptic nerve terminal. This fusion process is triggered by the presence of Ca^{2+} ions. SNARE proteins are also vital for the fusion of secretory vesicles, transported from the golgi body, with the plasma membrane, shown in Figure 1.5 (Sudhof, 2004).

References

Bennett, M., Scheller, R. (1994). A molecular description of synaptic vesicle membrane trafficking. *Ann. Rev. Biochem.* **63**, 63-100.

Biswas, R., Kuhne, H., Brudvig, G.W., Gopalan, V. (2001). Use of EPR spectroscopy to study macromolecular structure and function. *Science Progress* **84**(1), 45-68.

Fanucci, G.E., Cadieux, N., Kadner, R., Cafiso, D. (2003). Competing ligands stabilize alternate conformations of the energy coupling motif of a TonB-dependent outer membrane transporter. *Proc. Natl. Acad. Sci. U.S.A.* **100**(20), 11382-11387.

Hustedt, E.J., Beth, A.H. (1999). Nitroxide spin-spin Interactions: Applications to protein structure and dynamics. *Annu. Rev. Biophys. Biomol. Struct.* **28**,129-53.

Kleinsmith, L.J., Kish, V.M. *Principles of Cell and Molecular Biology*, 2nd ed., Harper Collins College Publishers: New York, 1995; 285, 761.

Knowles, P.F., Marsh, D., Rattle, H.W.E., *Magnetic Resonance of Biomolecules*, John Wiley & Sons: London, 1976.

Kweon, D.-H., Kim, C.S., Shin, Y.-K. (2002). The membrane-dipped neuronal SNARE complex: a site-directed spin labeling electronic paramagnetic resonance study. *Biochemistry* **41**(29), 9264-8.

Poirier, M.A., Wenzhong, X., Macosko, J.C., Chan, C., Shin, Y.-K., Bennett, M.K. (1998). The synaptic SNARE complex is a parallel four-stranded helical bundle. *Nature Struc. Bio.* **5**(9), 765-769.

Sudhof, T.C. (2004). The synaptic vesicle cycle. *Annu. Rev. Neurosci.* 27, 509-47.

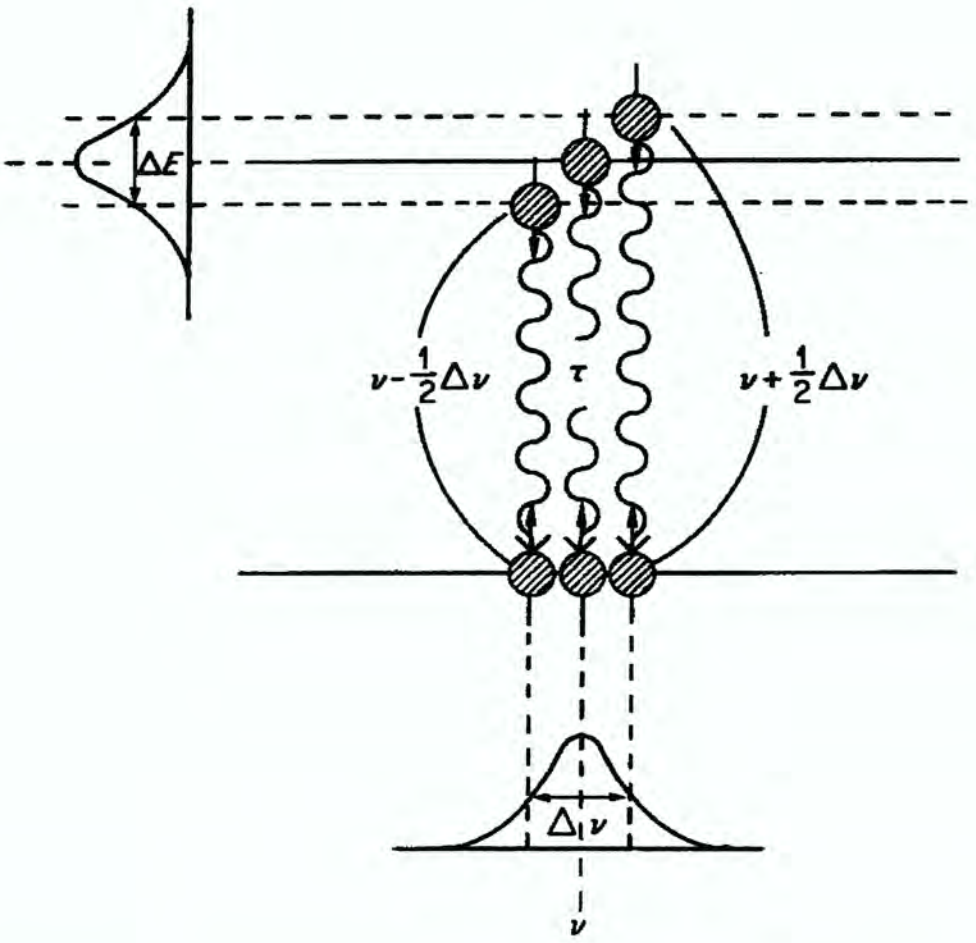

Figure 1.1. The energy from the ground state to the excited state of the electron spin is proportional to the frequency of the microwave radiation. Rather than Δν, EPR data is taken with respect the magnetic field, ΔB (Knowles *et al.*, 1976).

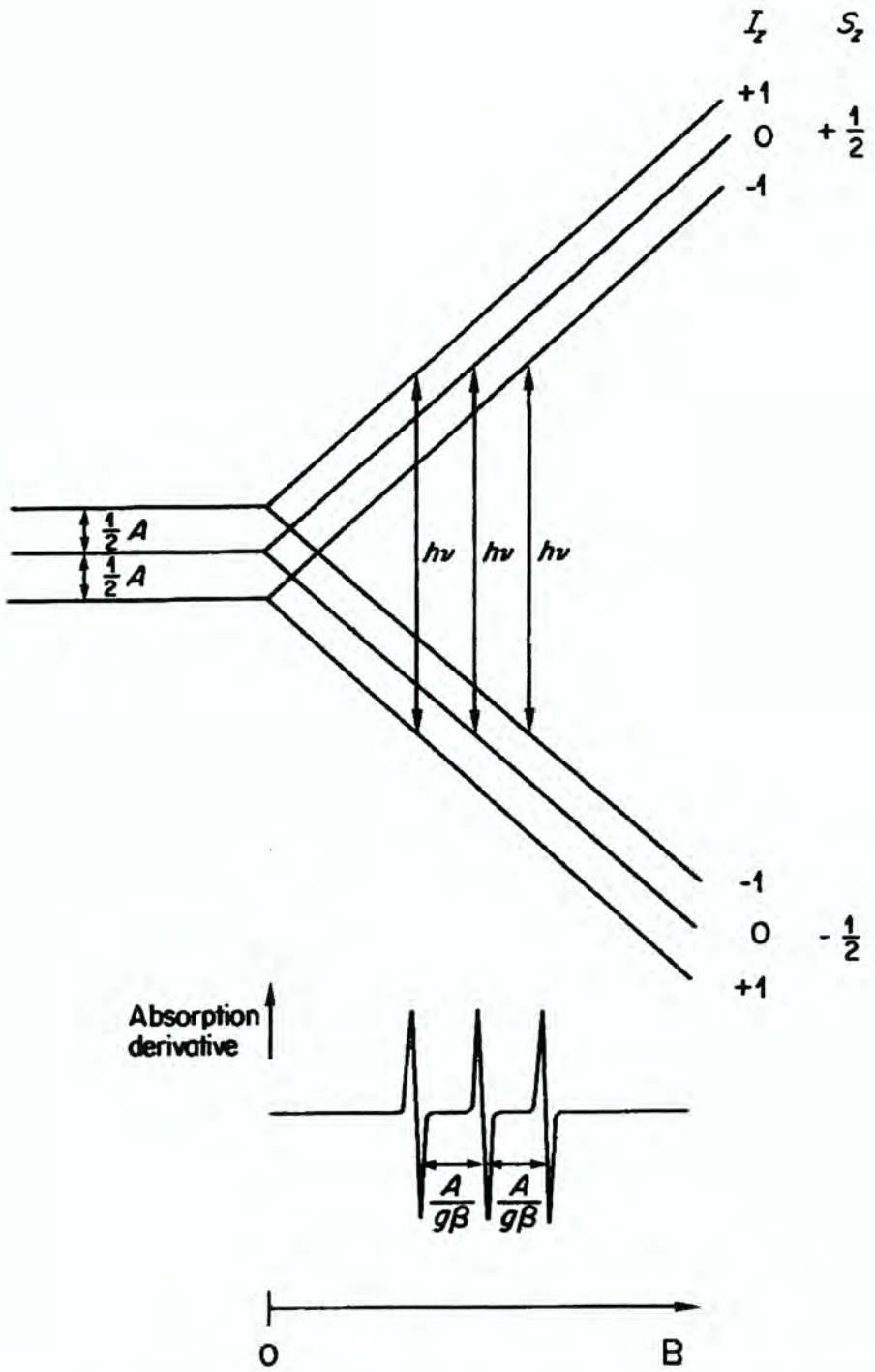

Figure 1.2. The three peaks of the EPR spectra of a nitroxide spin label represents the interaction of the unpaired electron the nuclear spin of its nucleus, nitrogen. The spectra in this figure was taken in the first derivative mode (Knowles *et al.*, 1976).

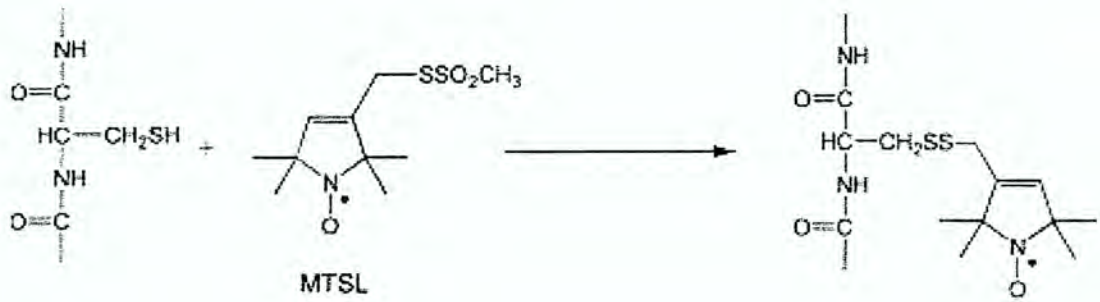

Figure 1.3. Site-directed spin-labeling (SDSL) is a chemical reaction between the sulfur of a cysteine residue in a protein and a sulfur of a nitroxide spin label, such as MTSL, forming a disulfide bond between the protein and the spin label at a cysteine mutated site in the protein (Fanucci *et al.*, 2003).

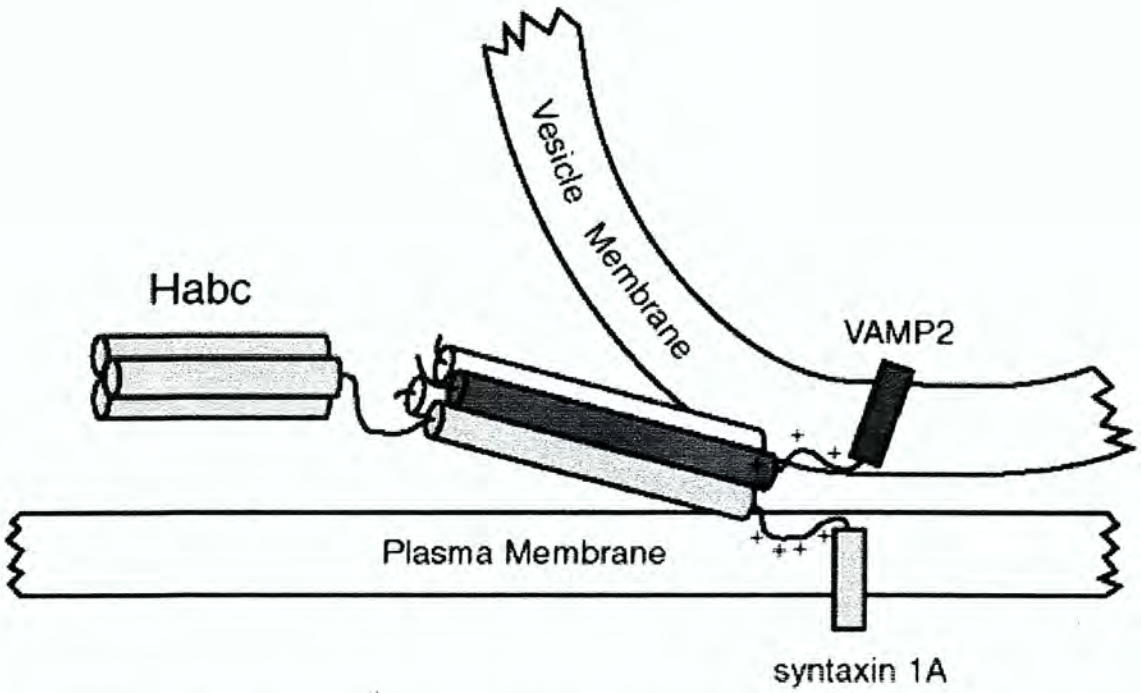

Figure 1.4. SNARE proteins are essential to membrane fusion within numerous parts of the biological cell. Syntaxin 1A is a transmembrane protein (t-SNARE), which interacts with a membrane surface protein SNAP-25 (t-SNARE) and VAMP-2 (v-SNARE), a transmembrane protein located on the opposing membrane, for membrane fusion and the release of the vesicle contents into the synaptic space between neurons. In this figure, SNAP-25 is represented by the white helices in the SNARE complex (Kweon *et al.*, 2002).

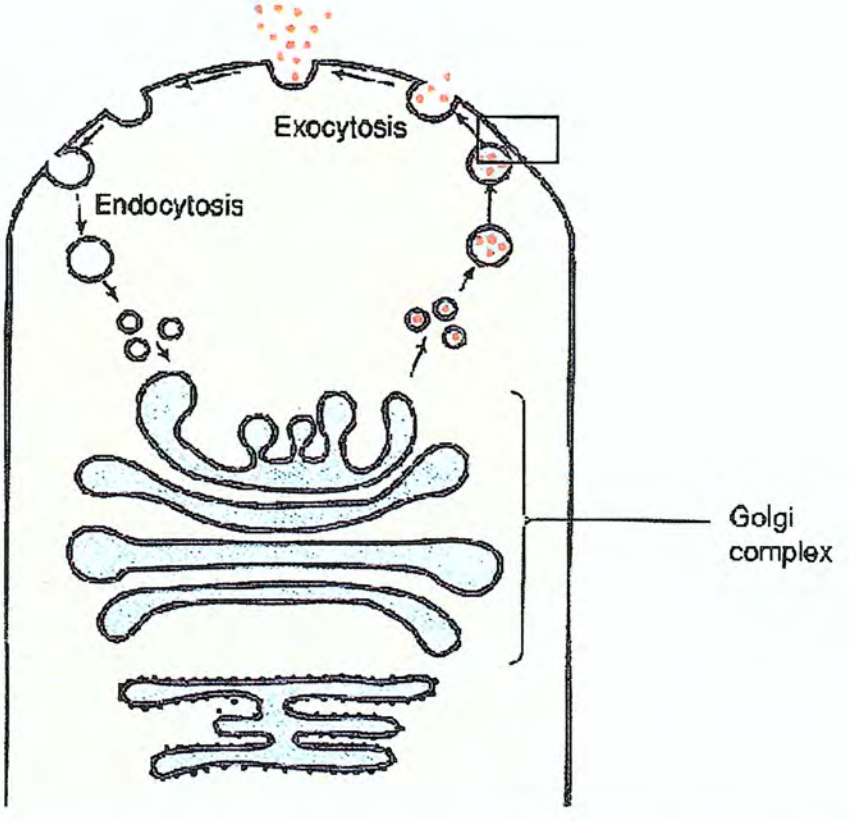

Figure 1.5. Vesicles from the golgi bodies fuse with the plasma membrane of a cell via SNARE complex formation (Kleinsmith & Kish, 1995).

CHAPTER 2: EXTENDING THE LIMITATIONS OF THE CONTINUOUS WAVE EPR SPECTROSCOPIC RULER

Introduction

Numerous methods of measuring distances using EPR data have been proposed in publications throughout the years. Each method has its limitations. Continuous wave (cw) EPR measurements are favorable at small distance increments, whereas pulse EPR methods are favorable at larger distances. Fourier deconvolution method accurately measures distances between 8 and 25 Angstroms. This cwEPR method takes advantage of the broadening due exclusively to dipolar interactions at low temperatures and deconvoluting the spectrum by subtracting a reference spectrum of a single spin with no dipolar interactions (Rabenstein & Shin, 1995). Peak height ratios and half-field transition methods are both good for measuring relatively short distances (Perrson *et al.*, 2001). Line-shape simulations accurately measure up to approximately 15 Angstroms (Hustedt & Beth 1999; Persson *et al.*, 2001). There are EPR methods that are capable of measuring distances beyond 25 Angstroms. These methods require pulse EPR spectroscopy, such as double electron-electron resonance (DEER) (Larson & Singel, 1993), the "2 + 1" pulse sequence (Raitsimring *et al.*, 1992), and double-quantum EPR (Borbat & Freed, 1999; Saxena & Freed, 1997).

The Fourier Convolution-Deconvolution Method

A protein labeled with two nitroxide spin labels may have spin-spin interactions. The spin-Hamiltonian contains a term for this dipole interaction, as well as a term for each spin

labeled residue not interacting with the other and a term for scalar spin exchange:

$$\hat{H} = \hbar\Omega_1 S_{1z} + \hbar\Omega_2 S_{2z} + \hbar^2\gamma_e^2(1-3\cos^2\theta)(3S_{1z}S_{2z}-S_1\cdot S_2)/2R^3 + \hbar J S_1 S_2$$

where $\hbar$ is Planck's constant ($h/2\pi$), γ_e is the gyromagnetic ratio of the electron, J is the spin exchange integral, S_1 is the spin of electron 1, Ω_1 is the resonance offset for electron 1, S_2 is the spin of electron 2, Ω_2 is the resonance offset for electron 2, θ is the angle between the interspin vector and the direction of the magnetic field, and R is the distance between the spin labels. The subscript z refers to the z-component of a spin. It is assumed that the dipole interaction term will be dominant when R is between 7 and 25 Angstroms (Xiao & Shin, 2000).

The resulting spectrum of a doubly spin-labeled protein is a convolution of (1) the spins interacting with each other, D(R, B'-B) and (2) a spin label interacting with its local environment, S(B).

$$\Pi(B) = \int_{-\infty}^{\infty} S(B)D(R,B'-B)dB'$$

D(R,B'-B) represents the dipolar broadening (interacting) spectrum and S(B) represents the non-interacting component of the spectrum. In reality, there is a distribution of distances between the spins, P(R), due to the flexibility of the nitroxide spin label after bonding to the protein, as well as to various conformations that a protein may adopt. Therefore, the dipolar interaction should be viewed as a weighted sum, M(B):

$$M(B) = \Sigma_R P(R)D(R,B).$$

With this in mind, the new equation representing the spectrum of a doubly labeled protein would be

$$\Pi(B) = \int_{-\infty}^{\infty} S(B')M(B'-B)dB'.$$

In Fourier space, the convolution of the interacting and non-interacting spins (Figure 2.1) would be represented as

$$\Pi(\omega) = S^*(\omega) \cdot M^*(\omega).$$

In order to "deconvolute" the spectrum, first it should be determined what part of the spectrum is the result of the non-interacting spin label. The inverse Fourier transformation of $\Pi^*(\omega)/S^*(\omega)$ would result in the the dipolar broadening function of the interacting component of the spectrum,

$$M(B) = (2\pi)^{-1/2} \exp\{2\pi i\omega[\Pi^*(\omega)/S^*(\omega)]\},$$

where ω is in units of $\pi/1024$ Gauss^{-1}.

In order to reduce the noise, the dipolar broadening function would be fit to the sum of two Gaussian functions. Performing an inverse Fourier tranformation of the best fit sum of functions yields a final dipolar spectrum, a Pake pattern (Figure 2.2). The Pake pattern has a splitting twice the qauntity of the magnetic field, 2B, and the average of this splitting is related to the distance between the spin labels, as shown in the equation below.

$$\langle 2B \rangle = (0.75)(3/2) g_e \beta R^{-3}$$

The distance between the two spin labeled amino acids can be determined by solving for "R" (Figure 2.3):

$$R = [(0.75)(3/2) g_e \beta / \langle 2B \rangle]^{1/3}$$

The scalar spin exchange (J-coupling) of the spins would be neglible because the spins are too far apart to experience through bond interactions. J-coupling would be the dominant term in the energy of the system if sites spin labeled were on adjacent residues or practically on top of one another. The non-interacting spins do contribute to the EPR spectrum. However, to eliminate the effect of the non-interacting spins on the final spectral

analysis the spectrum containing the spin interaction is divided by the reference spectrum (non-interacting spins) in Fourier Space. Therefore in the Hamiltonian given above the dipolar interaction would be the dominant term (Rabenstein & Shin 1995; Xiao & Shin, 2000).

The largest source of error when using this method is the presence of monoradical impurities from incomplete spin labeling of the doubly spin labeled sample. This problem can be taken care of mathematically by applying a δ-function to the equation coefficient for the population of monoradical impurities. The population of monoradical impurities is attained by the y-axis offset of the Gaussian function fitting to the data (Figure 2.1) (Berliner, *et al.*, 2000; Rabenstein & Shin 1995).

The population of spins is random isotropic (no orientation dependence). It is assumed that the anisotropy from the g- and A-tensors are negligible. However, under frozen conditions the various static orientations of these tensors give rise to homogeneous and inhomogeneous broadening in both spectra. Linewidth at half height is inversely proportional to spin-spin relaxation time.

$$\Delta B = (\pi T_2)^{-1}$$

The spin-spin relaxation time, T_2, is the time it takes for spins to relax back to ground state after one spin has become close enough to another spin to induce a change to a higher energy spin state (Figure 2.4). Spins that are close to one another have short spin-spin relaxation times, causing the linewidth to broaden (Knowles *et al.*, 1976).

Inhomogeneous broadening, T_2^*, is due to inconsistent magnetic field strength throughout the sample cavity. It gives Gaussian shaped linewidths.

$$\Delta B = (\pi T_2^*)^{-1}$$

This type of broadening is often seen in solid-state or motionally frozen samples that contain anisotropic (orientation dependent) magnetic interactions. Solid or frozen samples contain various tensor orientations which each yield a different frequency in a spectrum. Therefore rather than one sharp peak for each tensor orientation, the peaks appear as one broad band, referred to as a powder pattern. On the other hand, fast motions of the tensors, such as rapid molecular tumbling seen in solution state samples at higher temperatures, average out the anisotropic magnetic interactions, yielding a narrow linewidth. The Hamiltonian can now be adjusted to take anisotropy into account.

$$\hat{H} = \beta e B_0 \cdot \mathbf{g_1} S_{1z} + \beta e B_0 \mathbf{g_2} S_{2z} - \omega_n(I_{1z} + I_{2z}) + I_{1z}\mathbf{A_1}S_{1z} + I_{2z}\mathbf{A_2}S_{2z} + S_{1z}\mathbf{D}S_{2z} + JS_{1z}S_{2z}$$

D is the dipolar coupling tensor, J is the scalar exhange interaction, ω_n is the Larmor frequency of the nitrogen nucleus of the nitroxide spin label, and βe is the Bohr magneton. The A-tensor represents the interaction between the electron spin and the spin of the nucleus, I_z. The g-tensor represents the interaction between the electron and the DC magnetic field, B_0 (Hustedt & Beth, 1999). The magnetic field has no effect on the A anisotropy tensor; therefore this tensor has little effect on line broadening. The magnetic field strength directly affects the g anisotropy tensor and so it is this tensor that has the greatest impact on inhomogeneous broadening.

With the Fourier deconvolution method, spectra of samples are typically taken at -130°C to alleviate any incomplete time averaging of θ. At this low temperature molecular motions are slow and the tumbling rate is practically zero. Under these conditions, an anisotropic term would contribute greatly to the double spin labeled Hamiltonian energy operator. Below 7 Angstroms, J coupling is the dominant interaction. However, dipolar coupling dominates the spin label Hamiltonian between 7 and 25 Angstroms. Anisotropy

tensors may be cancelled out by reference to a singly labeled spectrum and the Fourier deconvolution method is a valid distance measurement technique. However, larger spin-spin interaction distances decrease the contribution of the dipolar coupling term to the energy of the system, enabling g-anisotropy to play a larger role for line broadening (Hustedt & Beth, 1999). This inhibits the ability of distances larger than 25 Angstroms to be measured accurately using the Fourier deconvolution method.

The protein and spin label are motional frozen and have very little flexibility at -130°C (143K). In theory, if the distance measurement was taken at -40°C, the protein would still have limited motion. Therefore incomplete time average of θ should not be a concern. However, the spin label would be more flexible. Increasing the mobility of the spin label would decrease the g-tensor anisotropy. This scenario may decrease the inhomogeneous broadening enough to determine the broadening due to dipolar coupling.

To test this theory, a double cysteine mutant was made on the neuronal v-SNARE, soluble SNAP-25[C] at positions M146C & M167C (Figure 2.5). The residues were 21 amino acids apart from one another ($i + 21$). Formation of the SNARE complex induces an alpha helical structure. Based on calculations of 3.6 residues per turn, 5.4 Angstroms per pitch, and 21 residues apart, the spin labels, in theory, would be separated by 32.4 Angstroms (Figure 2.6).

Methods

DNA Mutagenesis. Plasmid for Syntaxin, SNAP-25[C] & [N], and VAMP was attained from colleagues and transformed with DH5α subcloning efficiency cells. Mutant primers encoding sequences of SNAP-25[C] M146C & M167C were inserted separately in

Escherichia coli as N-terminal glutathione S-transferase (GST) fusion protein templates from the pGEX vectors and generated by polymerase chain reaction (PCR) based mutagenesis. There were no naturally occurring cysteine residues that needed to be mutated in SNAP-25[C]. A Quickchange site-directed mutagenesis kit (Stratagene) was used to generate the mutants. To create the doubly mutated DNA, the first amplified and verified mutant primer was used as the "template" and added to the second primer for PCR amplification. The double mutants were also verified by the DNA sequencing facility at Iowa State University. Wildtype and mutated DNA plasmid sequence alignment was done using the DNA sequence alignment query available at the Institut de Genetique Humaine website (Pearson *et al.*, 1997).

Purification of GST-fusion Proteins. The cDNA of soluble wildtype Syntaxin 1a (residues191-266), VAMP-2 (residues 1-94), and SNAP-25[C] (residues 125-206), with cysteine mutations at positions M146 & M167, was transformed with BL21 CodonPlus competent RIL cells, purchased from Stratagene (La Jolla, CA) and plated on luria broth agar plates containing of 0.1% ampicillin. A colony from this plate was inoculated into 10mL luria broth (LB) containing 10μL of 100 mg/mL ampicillin and 10μL of 30 mg/mL chloroamphenicol. The preculture was incubated for 16 hrs overnight at 37°C at 220 rpm. The cells were transferred to 600 mL of LB containing 3mL of 40% glucose. When the cells had an optical density (OD) of 0.6-0.8 the proteins within were overexpressed with 600uL 1M isopropyl-β-D-thigalactopyranonside (IPTG). The cells were incubated at 16°C for Syntaxin & VAMP-2, 20°C for SNAP-25[C]), 120 rpm for 4–6 hrs. The cells were

centrifuged at 6K rpm for 10 minutes. The supernatant was disposed of and the pellet was frozen at -80°C.

The frozen pellet was later defrosted at -4°C. 10mL of phosphate buffered saline (PBS) buffer pH 7.4, 40μL 500mM ethylenediaminetriacetic acid (EDTA), 100 μL of 200μM 4-(2-aminoethyl)benzenesulfonyl (AEBSF), 40μL of 0.4% Triton, and 0.5mL of 10% *n*-lauryl sarcosine were added and the solution was vortexed and sonicated to break the cell membrane. The broken cells were mixed for 30 minutes at 4°C and centrifuged at 15K for 20 minutes. The supernatant was added to a flash column containing 2.5–3 mL of nickel agarose beads and allowed to nutate at 4°C for at least 2 hrs. The beads were washed with a PBS buffer at least 3 times and thrombin cleavage buffer (TCB) pH 8 at least twice.

For cysteine mutated proteins, 50μL of 1M dithiothreitol (DTT) was added before sonicating, 40μL of 1M DTT was added to the supernatant before adding broken cell solution to the flash column, and 5μL of 1M DTT was added for every 1mL total solution in the flash column. The solution was allowed to nutate at least one hour. The column was washed with PBS pH 7.4 buffer 6 times. 80μL of 50mM methanethiosulfonate spin label (MTSL) was added to approximately 5 mL of total buffer and beads solution. Column nutated at room temp for 3–4 hrs. 80μL more of 50mM MTSL was added to column and allowed to nutate overnight at 4°C. Column was washed 3 times with PBS buffer and 2 times with TCB pH 8 buffer.

Approximately 4 mL of TCB was added to the column with 30μL of bovine thrombin and allowed to nutate at room temperature for approximately 40–60 minutes. The elution was mixed with a final concentration of 10% glycerol and stored at -80°C.

Purification of His_6-tagged Proteins. The cDNA of soluble wildtype SNAP-25[N] (residues 1-82) was transformed with BL21 CodonPlus efficiency cells and plated on luria broth agar plates containing 0.1% kanamycin. A colony from this plate was inoculated into 10mL luria broth containing kanamycin and chloroamphenicol. The preculture was incubated for 16 hrs overnight at 37°C at 220 rpm. 600 mL LB containing 0.1% kanamycin and 3 mL 40% glucose was then inoculated with the overnight culture and incubated at 37°C and 175 rpm. When the cells had an OD of 0.6–0.8 the proteins were then overexpressed with 600μL of 1M IPTG. The glucose is a source of food for the cells to grow. Lactose is naturally produced by the cells. However, this lactose is needed for overexpression of the protein. Therefore, glucose is added to preserve the lactose for the overexpression step of the purification. IPTG is a derivative of lactose and is added for the cell to overexpress the protein of interest. The cells were incubated at 16°C and 120 rpm for 4–6 hrs. The cells were then centrifuged at 6K rpm for 10 minutes. The supernatant was disposed of and the pellet was frozen at -80°C.

The frozen pellet was later defrosted at -4°C. 10mL of lysis buffer (10mM imidizole), 100μL of 100mM 4-(2-Aminoethyl)-benzenesulfonyl fluoride, hydrocholoric acid (AEBSF), and 500 μL of 10% (w/v) *n*-lauryl sarcosine were added. AEBSF is a protease inhibitor that prevents protease enzymes from cleaving peptide bonds. *N*-lauryl sarcosine helps to break apart the cell membrane. The solution was vortexed and sonicated to break the cell membrane. The broken cells were mixed for 30 minutes at 4°C and centrifuged at 13.5K for 20 minutes. The supernatant was added to a flash column containing 2.5–3 mL of Ni agarose beads and allowed to nutate at 4°C for at least 2 hrs. The beads were washed with a

wash buffer (20mM imidizole) at least 3 times. One small amount of SNAP-25[N] was eluted with eluent (250mM imidizole) for concentration and SDS-PAGE assays. The remainder was stored -80°C with the SNAP-25[N] still on the Ni agarose beads so that the SNARE complex may be formed when Syntaxin, SNAP-25[C] and VAMP-2 were added to the Ni column with SNAP-25[N] already bound.

The purity of all protein eluents were verified using a sodium dodecyl sulfate polyacridamide gel electrophoresis (SDS-PAGE) assay. The concentrations were checked using a BioRad protein assay kit using bovine serum albumin (BSA) as a standard. Spin labeling efficiency of SNAP-25[C] double and single mutants were calculated based on the relative concentration of a free radical standard, 4-hydroxy TEMPO. Glutathione agarose, bovine thrombin, n-lauroyl sarcosine, Triton X-100, dithiothrietol, ampicillin sodium salt, chloroamphenicol, kanamycin, and the low molecular weight size marker for SDS-PAGE were all purchased from Sigma.

EPR Spectrometer Parameters. A Bruker 300 continuous wave ESR spectrometer (Bruker, Germany) equipped with a low noise microwave amplifier (Miteq, Hauppauge, NY) and a loop-gap resonator (Medical Advances, Milwaukee, WI) was used. The modulation amplitude was set at 2 Gauss and an X-band (9.2 GHz) microwave frequency was used. Spectra were taken with 4 scans each of spin labeled SNAP-25[C] M146C/M167C alone and reconstituted into a soluble SNARE complex containing wildtype SNAP-25[N], VAMP-2, and Syntaxin. The sample cavity temperature was decreased with liquid nitrogen to -130°C (143 K), -60°C, and -40°C for binary complex samples. The distance measurements were performed with the spectra of ternary SNARE complexes taken at -40°C.

Results and Discussion

The spectra of the binary SNARE complex at -130°C, -60°C, and -40°C demonstrates the concept of inhomogeneous broadening (Figure 2.7). As the temperature decreases, inhomogeneous broadening increases due to the restricted motion of the g-tensor. Therefore g-tensor anisotropy is the major contributor to inhomogeneous broadening.

At room temperature, the left side of the spectra ($M_I = 1$) for the binary complex shows two peaks. The broad left peak represents the population of complexed SNARE and the narrow right peak the population for the non-complexed SNAP-25 [C] protein. In Figure 2.8b it can be seen that the population of non-complexed spin labeled protein (arrow) is greater than the population of complexed protein. Binary SNARE complex is fairly unstable and can dissociate easily. The ternary SNARE complex replaces one of the syntaxin proteins with VAMP-2, a vesicle associate protein (v-SNARE). This complex is very stable and does not dissociate easily. Therefore, in order to increase the amount of complexed protein and decrease the amount of non-complexed protein, samples used for distance measurement contained soluble VAMP-2 rather than twice the amount of syntaxin. The result of this change can be seen in Figure 2.8c. The ratio of complexed to non-complexed spin labeled SNAP-25[C] has increased. This can be seen from the change in peak heights on the left side of the spectra ($M_I = 1$) at room temperature. Figure 2.8a is the spectrum of SNAP-25[C] before it was placed in the SNARE complex.

While the overlay of the spectra for interacting and non-interacting spin labeled SNAP-25[C] appear to be different, there are other pieces of evidence that suggest the 32 Angstrom distance could not be measured by continuous wave EPR. First, when the distance

between the two spins can be measured, the data is fit to a Gaussian curve, as shown in the first two examples of Figure 2.9a. However, the data for 32 Angstroms appears to be a straight line rather than well fit to a Gaussian curve (Figure 2.10b), similar to the third example of Figure 2.10a. This suggests the distance between spin labels was not accurately measured. Second, the ω cutoff should not effect the distance measurement. However, it can be clearly seen from Figure 2.10 that the noise cutoff value made a significant difference in the calculated distance. These results indicate a 32 Angstrom distance could not be measured using the Fourier-deconvolution method at -40°C.

In theory, the non-interacting spectrum could be broadened by convoluting it with a Gaussian function until it closely resembles the interacting spectrum. This data analysis was attempted using the MatLab data program and shown in Figure 2.11. The non-interacting spectrum could not be broadened to match the interacting spectrum. Figure 2.12 shows the broadened non-interacting spectrum (dark blue) to be fit to the sides of the $m_I = 1$ peak and the center $m_I = 0$ peak of the interacting spectra (red). However, the top of the side peaks, $m_I = 1$ and -1, do not match well. If the difference between the interacting and non-interacting spectra were due to the broadening that would result from dipolar interactions or anisotropy tensors, the peaks would match up when the reference spectrum was broadened by convoluting the non-interacting spectrum with a Gaussian function.

This analysis indicates the difference between the two spectra is not broadening but rather a shift in peak positions of the hyperfine lines, which may be the result of different sample conditions. The non-interacting sample was the doubly spin labeled soluble SNAP-25[C] alone in solution with a random coil conformation. The interacting spin labeled sample was the same doubly labeled soluble SNAP-25[C] in complex with soluble Syntaxin

1a and soluble VAMP-2. In the SNARE complex, SNAP-25[C] is an α-helix. This is a different secondary structure than in the reference sample. The spin labels are at the "f" position of the coiled coil, therefore the substituted residues should not have tertiary interactions as a result of complex formation. These may or not be the cause of the shifted peaks seen in Figure 2.11.

The reference sample should be similar in conditions to the interacting sample to get the best distance measurement possible. More than one variable between the reference and doubly spin labeled samples may make a difference for measurement of larger distances.

Conclusions

Our experiment demonstrated that a 32.4 Angstrom distance could not be measured by continuous wave EPR spectroscopy at -40°C. The reason for this can only be speculated. Perhaps the anisotropy term in the Hamiltonian was not decreased enough for the dipolar interaction to be the dominant factor. On the other hand, perhaps having more than one variable between the reference and the interacting samples had an effect on the ability of the Fourier deconvolution method to accurately measure the distances larger than 25 Angstroms. In future experiments the reference sample should be a singly labeled soluble SNAP-25[C] that is in complex with the other SNARE proteins to reduce the number of variables between the reference and doubly labeled samples.

References

Borbat, P.P., Freed, J.H. (1999). Multi-quantum ESR and distance measurements. *Chem. Phys. Lett.* **313**, 145-154.

Hustedt, E.J., Beth, A.H. (1999). Nitroxide spin-spin interactions: Applications to protein structure and dynamics. *Annu. Rev. Biophys. Biomol. Struct.* **28**, 129-53.

Knowles, P.F., Marsh, D., Rattle, H.W.E., *Magnetic Resonance of Biomolecules*, John Wiley & Sons: London, 1976.

Larsen, R.G., Singel, D.G. (1993). Double electron-electron resonance spin-echo modulation: Spectroscopic measurement of electron spin pair separations in orientationally disordered solids. *J. Chem. Phys.* **98**, 5134-5146.

Ottemann, K., Thorgeirsson, T.E., Kolodziej, A.F., Shin, Y.-K., Koshland, D.E. (1998). Direct measurement of small ligand-induced conformational changes in the aspartate chemoreceptor using EPR. *Biochemistry* **37**, 7062-1069.

Pearson, W.R., Wood, T., Zhang, Z. Miller, W. (1997). Comparison of DNA sequences with protein sequences. *Genomics* **46**, 24-36.

Perrson, M. Harbridge, J.R., Hammarstrom, P., Mitri, R., Martensson, L.-G., Carlsson, U., Eaton, G.R., Eaton, S.S. (2001). Comparison of electron paramagnetic resonance methods to determine distances between spin labels on human carbonic anhydrase II. *Biophysical* **80**, 2886-2897.

Poirier, M., Shin, Y.-K., Bennett, M. (1998). The synaptic SNARE complex is a parallel four-stranded helical bundle. *Nature Struct. Bio.* **5**(9), 765-769.

Rabenstein, M.D., Shin, Y.K. (1995). Determination of the distance between two spin labels attached to a macromolecule. *Proc. Natl. Acad. Sci. U.S.A.* **92**, 8239-8243.

Raitsimring A., Peisach, J., Lee, H.C., Chen, X. (1992) Measurement of distance distributions between spin labels in spin-labeled hemoglobin using an electron spin echo method. *J. Phys. Chem.* **96**, 3526-3531.

Saxena, S., Freed, J.H. (1997). Theory of double-quantum 2-dimensional electron-spin-resonance with application to distance measurements. *J. Chem. Phys.* **107**, 1317-1340.

Xiao, W., Shin. Y.-K. EPR Spectroscopic Ruler: The Method and its Application. In Biological Magnetic Resonance, Vol. 19: Distance Measurements in Biological Systems by EPR; Berliner et al., Ed.; Kluwer Academic/Plenum Publishers, New York, 2000; pp 249-276

Zhang, F., Chen, Y., Kweon, D.-H., Kim, C.S., Shin, Y.-K. (2002). The four helix bundle of the neuronal target membrane SNARE complex is neither disordered in the middle nor uncoiled at the C-terminal region. *J. Biol. Chem.* **277**(27), 24294-24298.

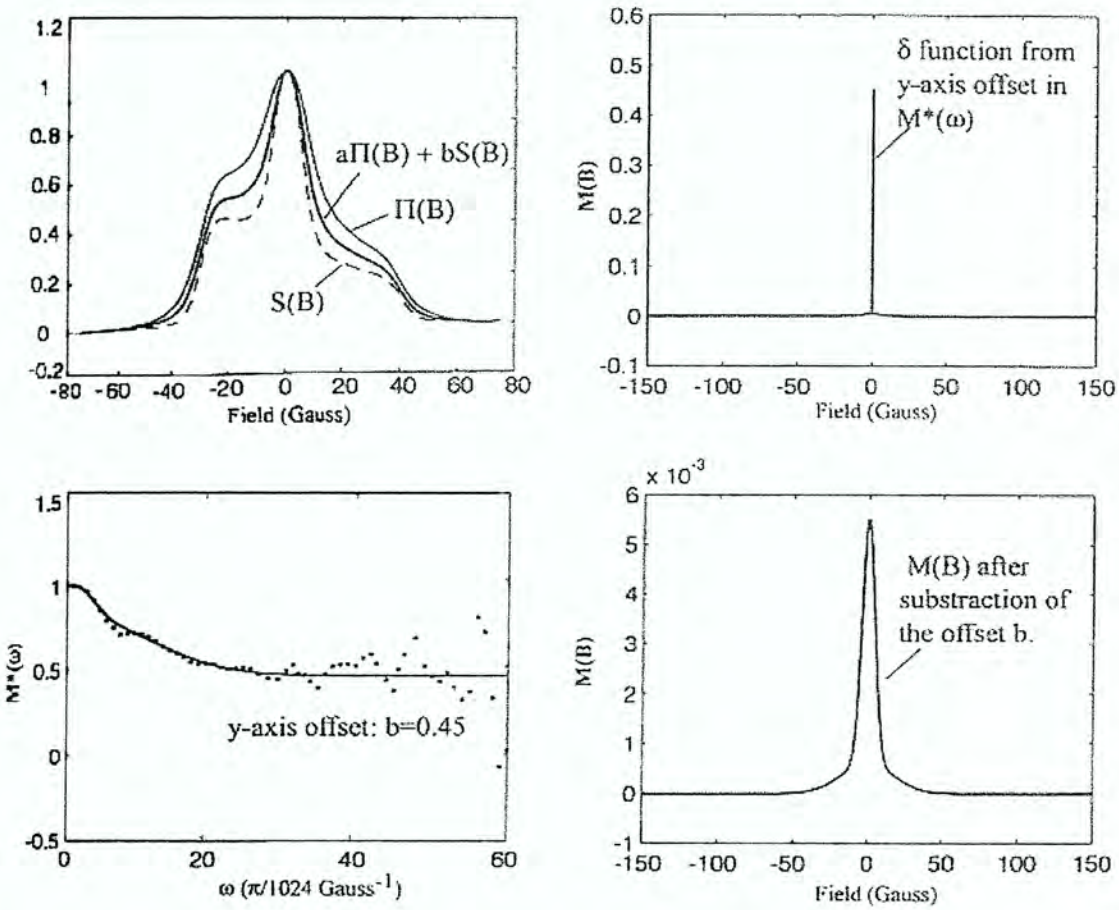

Figure 2.1. Fourier deconvolution theory subtracts the spectra of the reference from the spectra of the double spin labeled protein (Rabenstein & Shin, 1995).

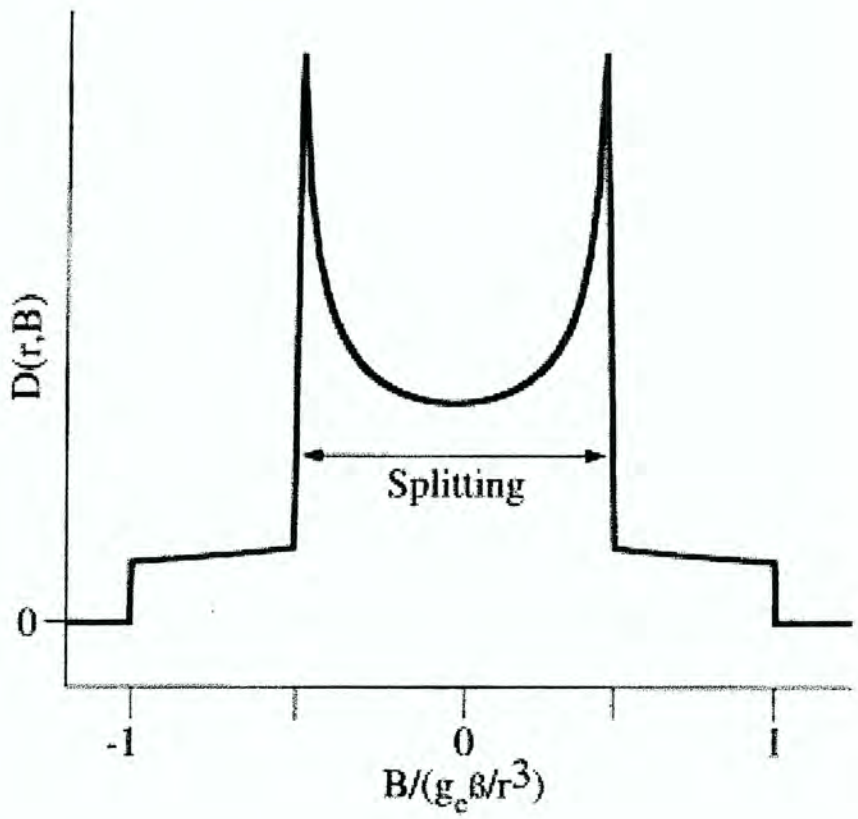

Figure 2.2. Pake Pattern splitting is twice that of the magnetic field and is inversely proportional to the distance between the two spin labels (Rabenstein & Shin, 1995).

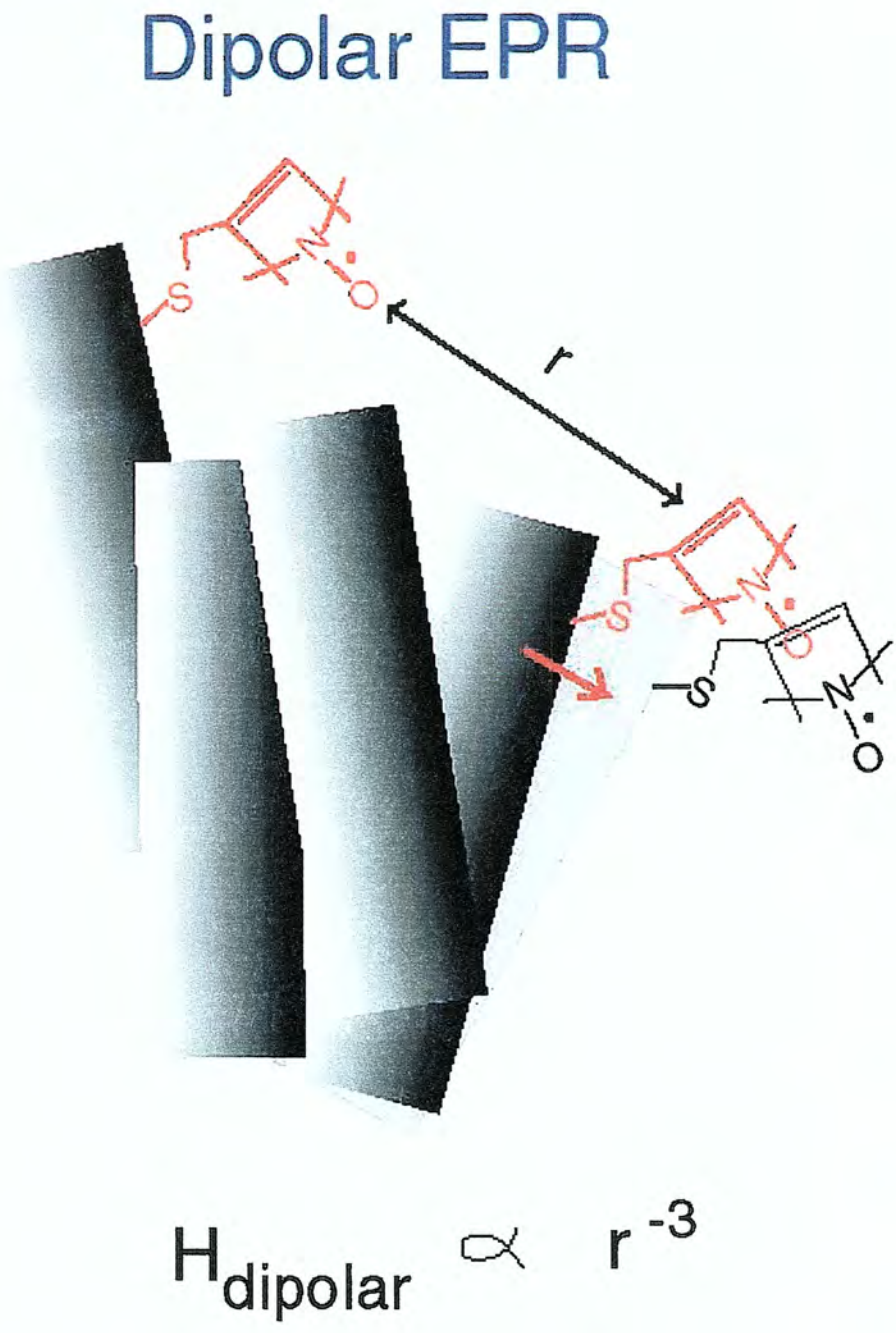

Figure 2.3. Dipolar EPR coupling measured using the Fourier deconvolution method (Rabenstein & Shin, 1995).

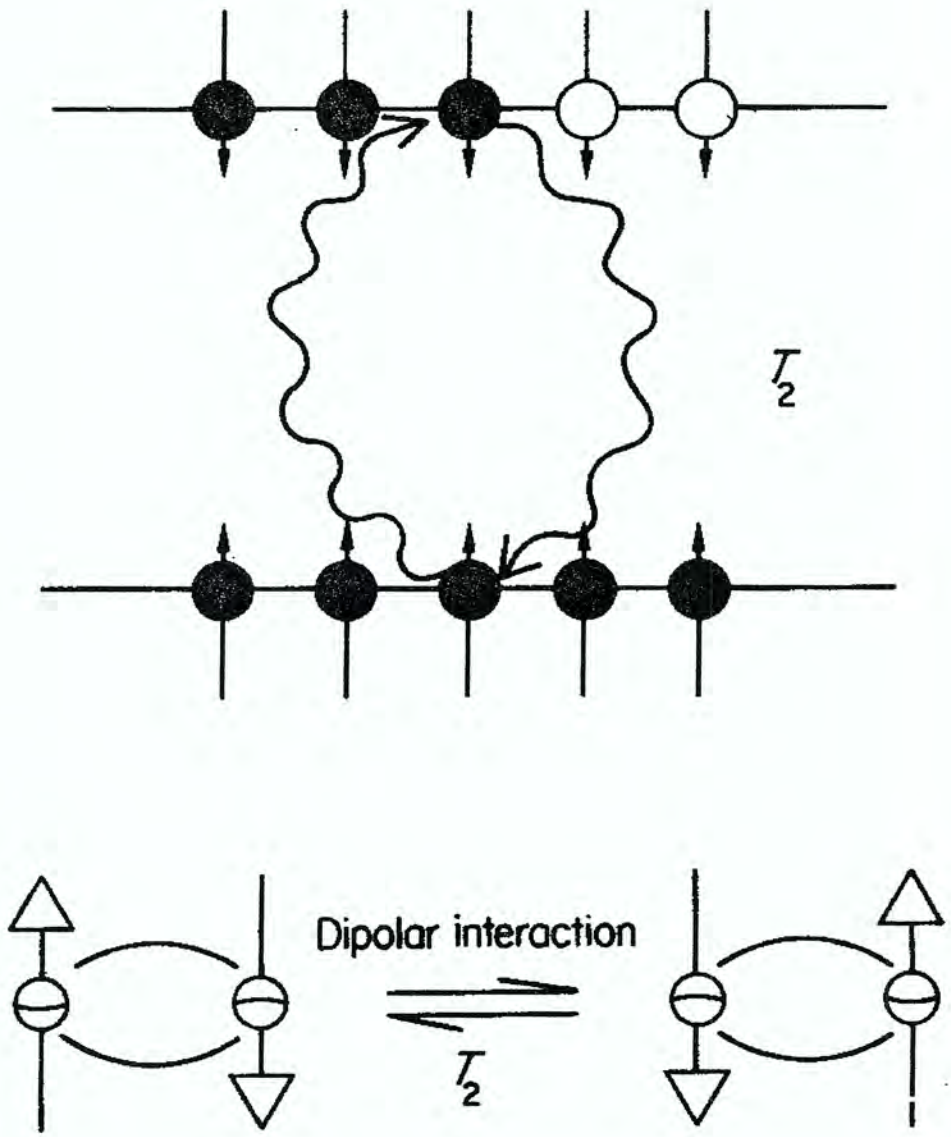

Figure 2.4. When one spin is close enough in vicinity to another, the dipolar interaction induces a change in spin states. The spin-spin relaxation time is referred to as T_2 (Knowles *et al.*, 1976).

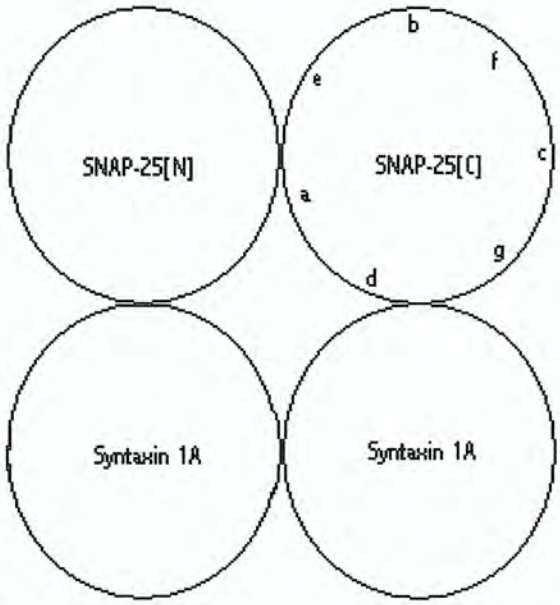

(a)

E	G	M	A	I	S	G	G	F	I	R	R	V	T	N	D	A
f	g	a	b	c	d	e	f	g	a	b	c	d	e	f	g	a
R	E	N	E	M	D	E	N	L	E	Q	V	S	G	I	I	G
b	c	d	e	f	g	a	b	c	d	e	f	g	a	b	c	d
N	L	R	H	M	A	L	D	M	G	N	E	I	D	T	Q	N
e	f	g	a	b	c	d	e	f	g	a	b	c	d	e	f	g
R	Q	I	D	R	I	M	E	K	A	D	S	N	K	T	R	I
a	b	c	d	e	f	g	a	b	c	d	e	f	g	a	b	c
D	E	A	N	Q	R	A	T	K	M	L	G	S	G			
d	e	f	g	a	b	c	d	e	f	g	a	b	c			

(b)

Figure 2.5. (a) The heptad repeat positions of amino acids within the binary SNARE complex that has a coiled coil conformation (adapted from Zhang *et al.*, 2002). (b) The amino acid sequence for soluble wildtype SNAP-25[C], showing heptad repeat positions of each residue. Residues highlighted red (M146 & M167) were mutated to cysteines.

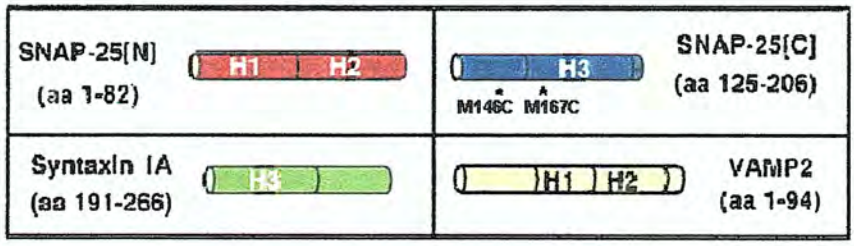

(a)

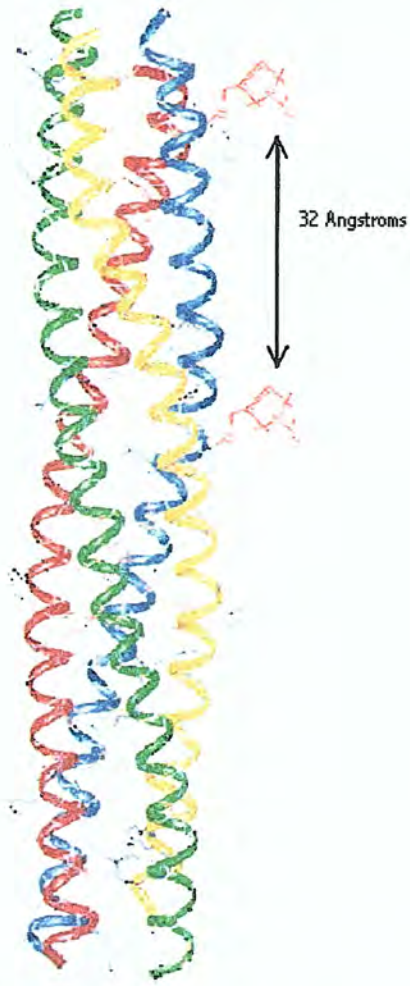

(b)

Figure 2.6. (a) Soluble neuronal SNARE proteins: Syntaxin, VAMP-2, SNAP-25[C], SNAP 25[N]. SNAP-25[C] was mutated at positions M146C & M167C. (b) The standard alpha helix contains 3.6 residues per turn. Therefore the estimated distance between spin labeled mutated sites would be approximately 32 Angstroms. (Both figures were adapted from Poirier *et al.* 1998)

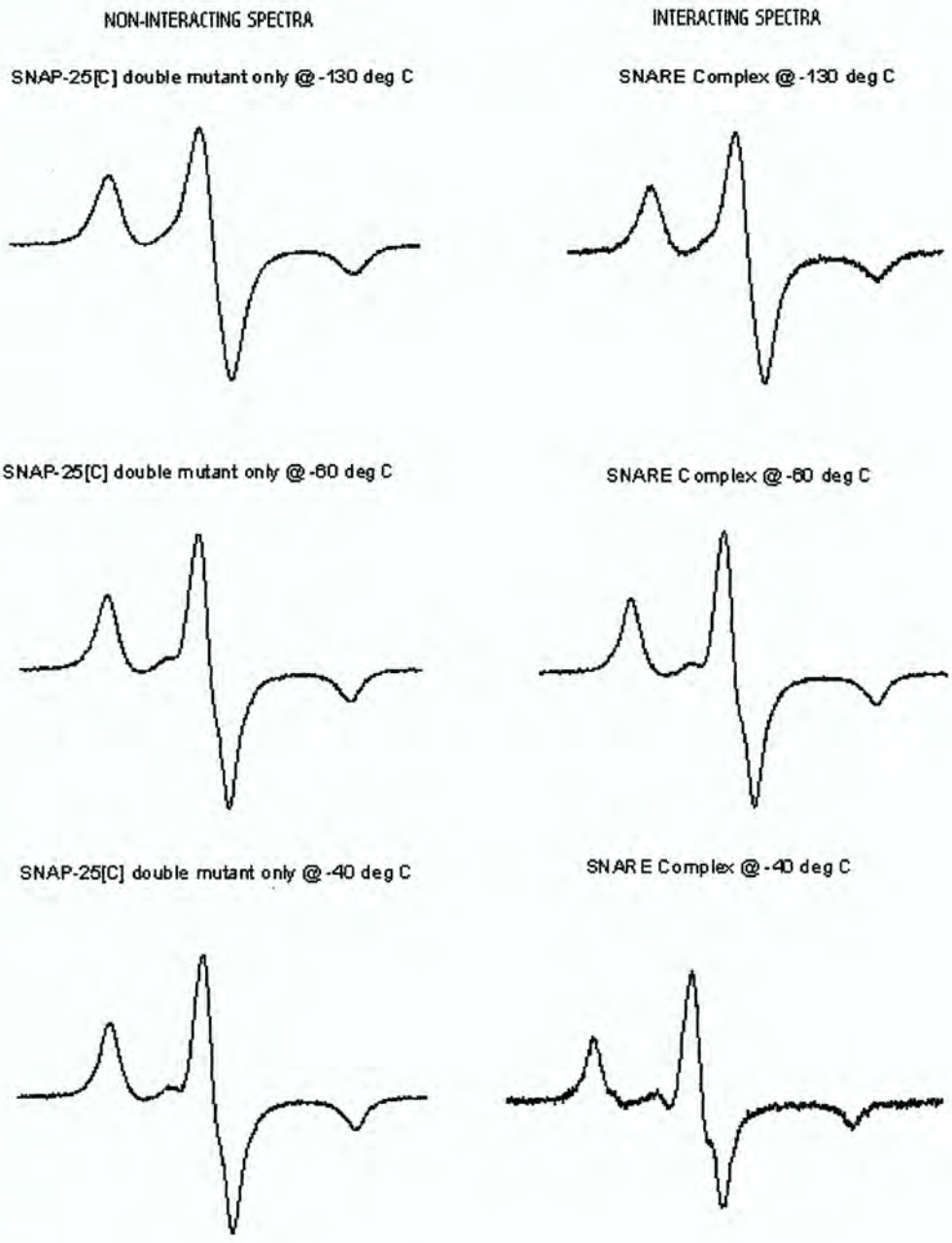

Figure 2.7. Demonstration of increasing linewidth as temperature decreases, using soluble binary SNARE complex. Anisotropic motions are averaged out at higher temperatures when the correlation time of the protein is fast. At lower temperatures, the correlation time is much slower and the anisotropic magnetic interactions cause the broadening of linewidths in the spectra.

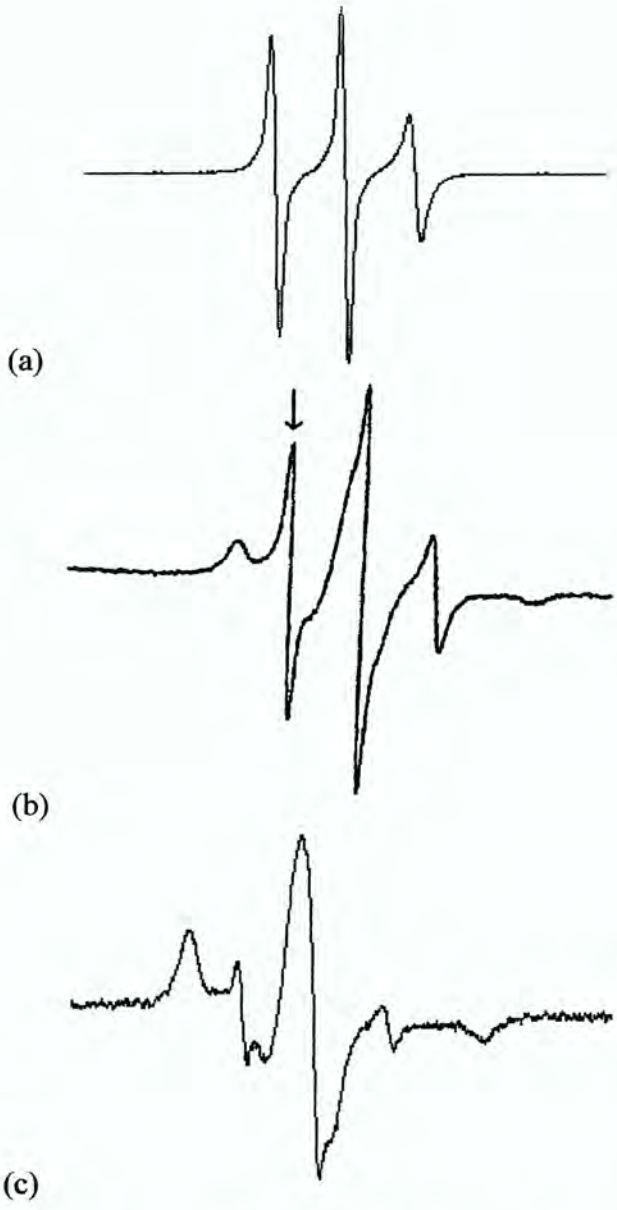

Figure 2.8. EPR spectra of spin-labeled SNARE at room temperature. (a) The EPR spectrum of double spin labeled SNAP-25[C]. The protein is in a random coil conformation and the spin labels are too far apart from one another to interact. The spin label efficiency was 100%, based on a relative calculation with a standard, 4-hydroxy TEMPO. (b) The EPR spectrum of double SDSL SNAP-25[C] in the binary SNARE complex, using two syntaxin molecules. (c) The EPR spectrum of double SDSL SNAP-25[C] in the ternary SNARE, using VAMP-2 instead of a second syntaxin molecule. Complex formation contains the soluble regions of wildtype Syntaxin 1A, SNAP-25[N] and VAMP-2.

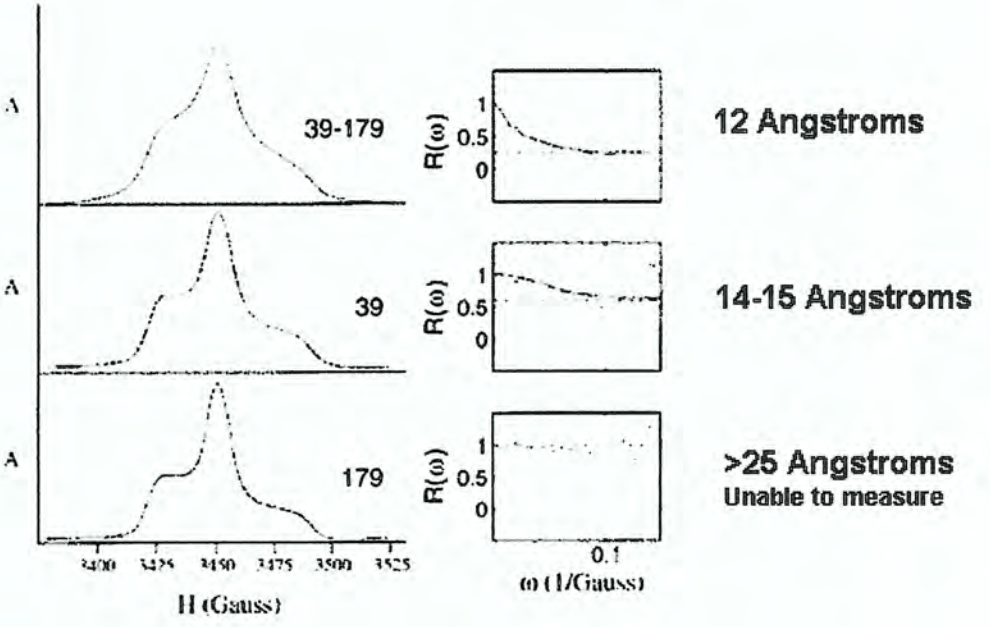

(a)

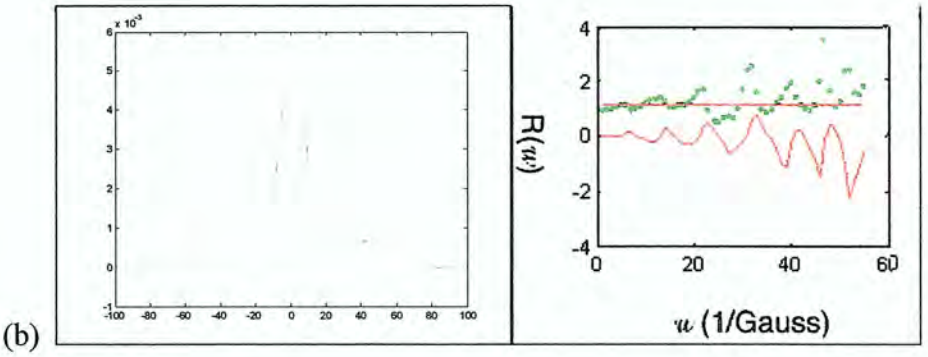

(b)

Figure 2.9. (a) Examples of distance measurements between spin labels using the Fourier deconvolution method (adapted from Ottemann *et al.*,1998). (Left b) Absorbance spectrum of non-interacting spin labels (red) compared to absorbance spectrum of interacting spin labels (green). (Right b) Fit data to two Gaussian functions. The intensity (y-axis) vs. units of inverse Gauss (x-axis) is linear, indicating it is unable to fit the data to a Gaussian function. The analysis was performed with MatLab 7.0.

Figure 2.10. The effect of different noise cutoffs (ω) on the overall distance measurement and for each of the Gaussian functions fit to the data.

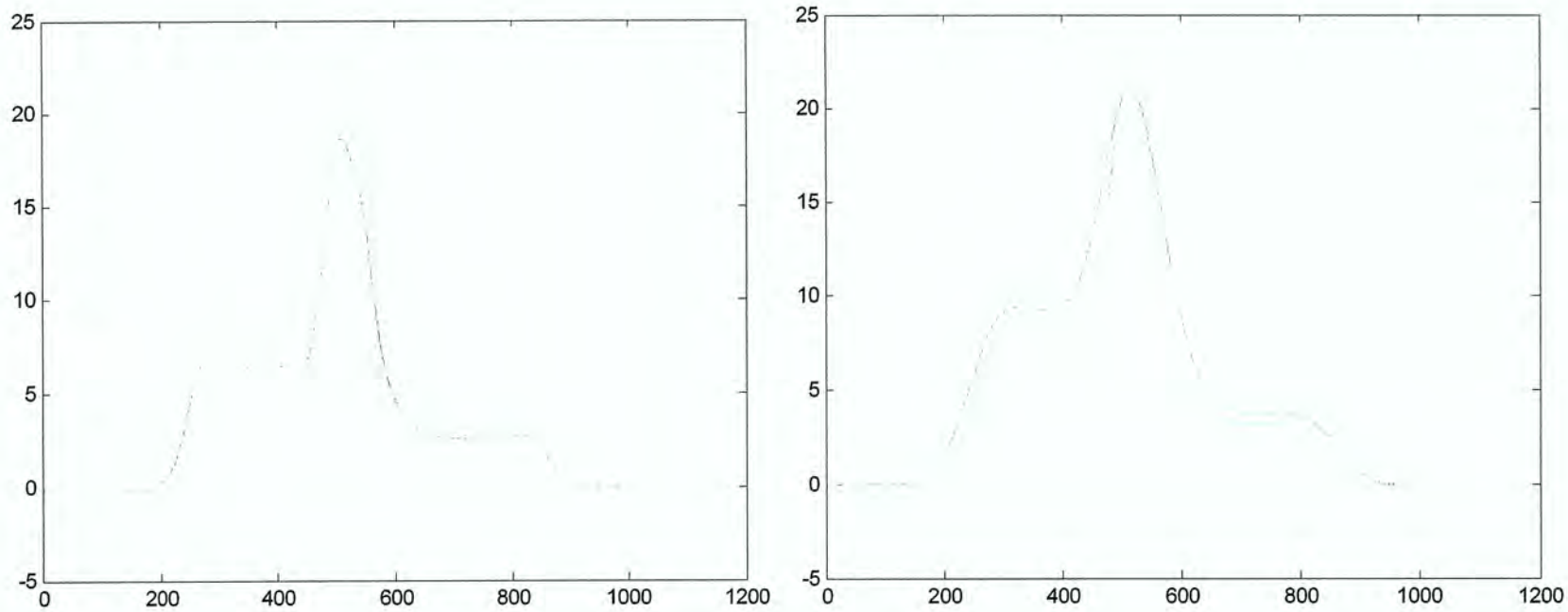

Figure 2.11. Data analysis on the amount of broadening and convolution necessary to broaden the non-interacting spectra (original spectra - light blue; broadened spectra - dark blue) to resemble the spectra of interacting spin labels (red). (a) The non-interacting spectrum was broadened 0.25 points, with a 0.8 y-axis scaling factor. (b) The non-interacting spectrum was broadened 35 points, with 0.9 y-axis scaling factor. The analysis shows the difference between the interacting and non-interacting spectra is not a matter of broadening due to anisotropy factors, but rather a "shift" that could be caused by secondary structure differences between the two systems. The analysis was performed with MatLab 7.0.Gugl.

CHAPTER 3: DETERMINING PROTEIN CONFORMATION USING THE EPR SPECTROSCOPIC RULER

Introduction

Protein conformation often reflects the function of a protein. Common conformations found in proteins are α-helices, 3_{10}-helices, β-sheets, and random coils. Particular traits characterize these different conformations. For example, an α-helix contains 3.6 residues (amino acids) per turn, and each of these turns are approximately 5.4 Angstroms in distance (one translation along the helical axis), and the length of an amino acid. Also, every residue within an α-helix is approximately 1.5 Angstroms in length (Nelson & Cox, 2000). A 3_{10}-helix is more tightly wound than an α-helix. This helix has 3 residues per turn and contains 10 atoms in the ring enclosed by the carbonyl-amine hydrogen bond. An α-helix would be considered a 3.6_{13}-helix (Monaco *et al.*, 1999). A β-sheet that is anti-parallel has a period length (2 amino acids) of 7 Angstroms. This is the optimum distance, with no forces pulling on the sheet. Therefore the length of one amino acid in a β-sheet can be approximated to 3.5 Angstroms. A random coil conformation has no definite structure (Nelson & Cox, 2000). With this knowledge, as well as the known number of residues between the spin labels, evidence of a local conformation within a protein can be obtained by comparing the experimental data with that of calculated distances expected for each possible conformation.

The yeast SNARE Sso1p is a transmembrane protein integrated into the target membrane (t-SNARE). The soluble region of this protein is known to conform to an alpha helical structure upon complex formation with the t-SNARE Sec9, a protein with a palmitoyl vesicle membrane attachment, and the v-SNARE Snc2. The section of Sso1p involved in the

SNARE motif ends at residue 250, and the transmembrane region of the protein begins around residue 267. The transmembrane section of Sso1p is assumed to be alpha helical, according to recent unpublished results by Y. Zhang and Y.-K. Shin. Residue K263 is located in the linker region of the protein, outside of the membrane. Residue V270 is located just within the transmembrane region. In order to determine the conformation of the region linking the soluble section of the protein to the transmembrane domain, a double cysteine mutant of full length Sso1p K263C/V270C is studied. The cysteine mutations are 7 amino acids apart.

If the conformation is helical, there would be 3.6 residues per turn, which means there would be 2 complete helical turns. There is a length of 5.4 Angstroms for a translation along the principal axis of one helical turn (Nelson & Cox, 2000). Therefore a distance measurement of ~10.8 Angstroms would be expected. The mutations would be at the same position of the helix and so the spin label "arm" at each mutated position would be eclipsed with the other. Therefore, the length of the "arm" should not affect the distance measurement if the conformation of the linker is alpha helical.

If the conformation is a beta sheet, the distance measurement would be the maximum length possible for amino acids 7 residues apart from each other. Each residue is approximately 3.5 Angstroms in length. Therefore if the conformation of the linker was a beta sheet, the distance measured between the spin labels would be approximately 24.5 Angstroms. If the conformation of the linker domain is a random coil, the distance measurement would be somewhat less than 24.5 Angstroms.

Methods

His_6-tagged Protein Purification. The cDNA of soluble wildtype Sec9 (residues 401-651) was transformed with Rosetta pLysS cells and plated on luria broth agar plates containing kanamycin. The Sec9 used in this study did not contain the first 400 amino acids of its N-terminal. However, these residues do not effect SNARE complex formation and so there is no concern over their presence. A colony from this plate was inoculated into 10mL luria broth containing kanamycin and chloroamphenicol. The preculture was incubated for 16 hrs overnight at 37°C at 220 rpm. 600 mL LB containing 0.1% kanamycin and 3 mL 40% glucose was then inoculated with the overnight culture and incubated at 37°C and 175 rpm. When the cells had an optical density (OD) of 0.6–0.8 the proteins were then overexpressed with 600μL isopropylthio-β-D-galactopyranoside (IPTG). The glucose is a source of food for the cells to grow. Lactose is naturally produced by the cells. However, this lactose is needed for overexpression of the protein. Therefore, glucose is added to preserve the lactose for the overexpression step of the purification. IPTG is a derivative of lactose and is added for the cell to overexpress the protein of interest. The cells were incubated at 22°C and 120 rpm for 4–6 hrs. The cells were then centrifuged at 6K rpm for 10 minutes. The supernatant was disposed of and the pellet was frozen at -80°C.

The frozen pellet was later defrosted at -4°C. 10mL of lysis buffer (10mM imidizole), 100μL of 100mM 4-(2-Aminoethyl)-benzenesulfonyl fluoride, hydrocholoric acid (AEBSF), and 500 μL of 10% (w/v) *n*-lauryl sarcosine were added. AEBSF is a protease inhibitor that prevents protease enzymes from cleaving peptide bonds. N-lauryl sarcosine helps to break apart the cell membrane. The solution was vortexed and sonicated to break the cell membrane. The broken cells were mixed for 30 minutes at 4°C and centrifuged at 13.5K

for 20 minutes. The supernatant was added to a flash column containing 2.5–3 mL of Ni agarose beads and allowed to nutate at 4°C for at least 2 hrs. The beads were washed with a wash buffer (20mM imidizole) at least 3 times. Approximately 4 mL of elution buffer (250mM imidizole) was added to the column and allowed to nutate at 4°C for approximately 1 hr. 25 μL of AEBSF was added to stop the reaction with thrombin. Besides acting as a protease inhibitor, AEBSF also acts as an inhibitor to thrombin. The elution was mixed with a final concentration of 10% glycerol and stored at -80°C. Glycerol is a commonly used cryoprotectant for proteins.

GST-fusion Protein Purification. The cDNA of soluble wildtype Snc2 (residues 1-115) was transformed with Rosetta pLysS cells and plated on luria broth agar plates containing ampicillin. A colony from this plate was inoculated into 10mL luria broth containing ampicillin and chloroamphenicol. The preculture was incubated for 16 hrs overnight at 37°C at 220 rpm. When the cells had an OD 0.6-0.8 the proteins within were overexpressed with 600uL IPTG. The cells were incubated at 22°C and 120 rpm for 4-6 hrs. The cells were centrifuged at 6K rpm for 10 minutes. The supernatant was disposed of and the pellet was frozen at -80°C.

The frozen pellet was later defrosted at -4°C. 10mL of PBS buffer, EDTA, AEBSF, and *n*-lauryl sarcosine (same molar amounts as Chapter 2 experiments) were added and the solution was vortexed and sonicated to break the cell membrane. The broken cells were mixed for 30 minutes at 4°C and centrifuged at 15K for 20 minutes. The supernatant was added to a flash column containing 2.5-3 mL of nickel agarose beads and allowed to nutate at 4°C for at least 2 hrs. The beads were washed with a PBS buffer at least 3 times and

thrombin cleavage buffer (TCB) at least twice. Approximately 4 mL of TCB was added to the column with 30μL of bovine thrombin and allowed to nutate at room temperature for approximately 40–60 minutes. The elution was mixed with a final concentration of 10% glycerol and stored at -80°C.

Purification of Spin-Labeled Sso1p Mutants. Mutants were made by laboratory colleague Yong Chen. Mutation primers were ordered from Qiagen. The mutations were made via polymerase chain reaction (PCR) with Sso1p plasmid and pGEX vector and verified by the Iowa State University DNA sequencing facility. The cDNA of full length Sso1p (residues 1-290) was copied with DH5α sublconing effeciency cells and transformed with Rosetta pLysS cells and plated on luria broth agar (LBA) containing ampicillin.

10 mL of autoclaved luria broth containing 0.1% ampicillin and 0.1% chloroamphenicol was inoculated with a colony from the Rosetta cell LBA plate. The preculture was incubated overnight for 16 hrs at 37°C at 220 rpm. The preculture was pipetted into 600 mL autoclaved LB containing 0.1% ampicillin, 0.1% chloroamphenicol, and 3 mL 40% glucose. The *E. coli* cells were harvested until they achieved an OD of 0.6-0.8. The proteins were overexpressed by the addition of 600μL 1M IPTG and incubated at 18° and 120 rpm for 4–6 hrs. The cells were centrifuged at 6K rpm for 10 minutes. The supernatant was disposed of and the pellet was frozen at -80°C.

The frozen pellet was later defrosted at 4°C. 10mL of PBS (phosphate buffered saline) buffer with 0.1% Triton-X at pH 7.4, and the molar amounts of AEBSF, lauryl sarcosine, EDTA, and DTT were added as in the experiments performed in Chapter 2. The solution was vortexed and then sonicated to break the cell membrane. The broken cells were

mixed for 30 minutes at 4°C and then centrifuged at 13.5K for 20 minutes. The supernatant was then added to a flash column containing 2.5–3 mL of glutathione-S-transferase (GST) beads and dithiothreitol (DTT). The protein solution nutated on the beads for at least 2 hrs and then was drained. The beads were then washed with the PBS buffer at least 5–7 times. In order to ensure that the cysteine residues remain reduced, DTT was added again, nutated at least 1 hr, and then washed with PBS buffer at least 6 times. Washing the beads to remove excess DTT is important because DTT would react with the nitroxide spin label, resulting in low spin labeling efficiency.

80μL of 50mM 1-Oxyl-2,2,5,5-tetramethyl-Δ3-pyrroline-3-methyl) methanethiosulfonate (MTSL), purchased from Toronto Research Chemicals (North York, Canada), was added to the column and allowed to nutate at room temperature for 4 hrs and then at 4°C overnight after 80μL more 50mM MTSL was added. The column was washed 3–4 times with PBS buffer and 3 times with thrombin cleavage buffer (TCB) containing 0.2% TritonX-100. With approximately 4 mL of buffer on the column, 30μL bovine thrombin was then added to the column and allowed to nutate at room temperature for 40–60 minutes. The protein was then eluted off the column and 25μL of 100mM AEBSF was added to the final yield. 80uL more of 50mM MTSL was added with urea (final concentration less than 1M) and nutated at room temperature for 3 hrs. An additional aliquot of MTSL was added and the solution was nutated overnight at 4°C. To remove the excess spin label and urea, the solution was dialyzed in TCB buffer using 3KDa dialyzing tubing. The dialyzing buffer was changed every 3–4 hrs and this was done at least 4 times. The elution was stored at -80°C with a final glycerol concentration of 10%. Sso1p K263C/V270C had a spin label efficiency of 76%.

The purity of all protein eluents were verified using a sodium dodecyl sulfate polyacridamide gel electrophoresis (SDS-PAGE) assay. The concentrations were checked using BioRad protein assay kit using bovine serum albumin (BSA) as a standard. Spin labeling efficiency of Sso1p double and single mutants were calculated based on the relative concentration of a free radical standard, 4-hydroxy TEMPO.

Preparation of Vesicles. The vesicles were composed of 1-palmitoyl-2-oleoyl phosphatidylcholine (POPC) with 15 mol % 1,2-dioleoyl phophatidylserine (DOPS), which were purchased from Avanti Polar Lipids (Birmingham, AL). The lipids in powder form were dissolved in chloroform in a disposable glass test tube. The chloroform was evaporated off with air under a hood, leaving the lipids adhered to the glass. The test tube was placed in a dessicator overnight. The lipids were dissolved in 1 mL of 25mM HEPES 100mM KCl pH 7.5 buffer and pushed through an extruder. The vesicles were stored at 4°C for a few days.

Reconstitution of Sso1p into Vesicle Membrane. Vesicles and spin-labeled Sso1p protein were mixed together and nutated at room temperature for approximately 15 minutes. Bio-Beads SM-2 adsorbent beads, purchased from Bio-Rad (Hercules, CA) were added to the solution for the purpose of adsorbing the Triton 100-X detergent in the solution. The bio-beads nutated at 4°C for 30 minutes, were centrifuged down and the solution was pipetted off into fresh beads. This was repeated three times.

SNARE Complex Formation. The Sso1p protein already reconstituted in vesicles was mixed with two times as much soluble Sec9 (wt, amino acids 401-651) and allowed to mix

for at least 5 minutes to form binary SNARE complexes. After spectra were taken, four times the amount of Snc2p (wt, amino acids 1-115) was added and mixed for at least 5 minutes for ternary SNARE complex formation to occur.

EPR Spectrometer Parameters. A Bruker 300 continuous wave ESR spectrometer (Bruker, Germany), equipped with a low noise microwave amplifier (Miteq, Hauppauge, NY) and a loop-gap resonator (Medical Advances, Milwaukee, WI) was used. The modulation amplitude was set at 2 G; the modulation frequency at 100 kHz. X-band (9.2 GHz) microwave frequency was used. The sample cavity temperature was decreased with liquid nitrogen to a temperature of -130°C (143 K). Spectra of Sso1p K263C reconstituted into vesicles and in the SNARE complex, as well as Sso1p K263C/V270C reconsituted and in complex, were taken with 4 scans at room temperature and 143 K (-40°C).

Results and Discussion

The Fourier convolution-deconvolution method yielded a distance measurement of 12–14 Angstroms between residues 263 and 270 of Sso1p. While 10.8 Angstroms would be the expected distance for a perfect α-helix, with spin labels at residues *i* and *i* + 7, should the conformation be "perfect" to be labeled an α-helix? Using a TOAC spin label, Monaco and colleagues (1999) determined a distance of 12.04 Angstroms for an α-helix with spin labels separated by 7 residues. They also determined the same amino acid separation would have a distance of 13.98 Angstroms in a 3_{10}-helix.

Hanson *et al.* (1996) argue that a 3_{10}-helix is a thermodynamic folding intermediate between a random coil and an α-helix. However, the 3_{10}/α-helix threshold are peptides of

approximately 8 residues. In addition, according to Zhang & Hermans (1994) and Tirado-Rives *et al.* (1993), a polyalanine α-helix was found to be lower in free energy by 10–16 kcal/mol than a polyalanine 3_{10}-helix. Therefore, it is improbable a 3_{10}-helix would exist in the linker region of a SNARE protein.

Current research is being done by Yinghui Zhang of the Shin laboratory at Iowa State University on the transmembrane domain of Sso1p. His findings estimate that the linker and transmembrane domains are helical in structure. More specifically his research suggests that the transmembrane domain is α-helical and the region from 263 to 265 of the linker region is unstructured (unpublished work).

Conclusions

The distance measurement yielded a length of 12–14 Angstroms. Based on comparing the results yielded by the Fourier deconvolution method with Fourier deconvolution distance measurements performed in the past, and the recent EPR collisional method experiments performed by the Shin laboratory, the linker region conformation is most likely an α-helix that is slightly unstructured between residues 263-265.

References

Hanson, P., Martinez, G., Millhauser, G., Formaggio, F., Crisma, M., Toniolo, C., Vita, C. (1996). Distinguishing helix conformations in alanine-rich peptides using the unnatural amino acid TOAC and electron spin resonance. *J. Am. Chem. Soc.* **118**, 271-272.

Monaco, V., Formaggio, F., Crisma, M., Toniolo, C., Hanson, P., Millhauser, G., George, C., Deschamps, J.R., Flippen-Anderson, J.L. (1999). Determining the occurrence of a 3_{10}-helix

and an α–helix in two different segments of a lipopeptaibol antibiotic using TOAC, a nitroxide spin-labeled C^{α}-tetrasubstituted α–aminoacid. *Biorg. Med. Chem.* **7**, 119-131.

Munson, M., Chen, U., Cocin, A.E., Schultz, S.M., Hughson, F.M. (2000). Interactions within the yeast t-SNARE Sso1p that control SNARE complex assembly. *Nature Struct. Biol.* **7**(10), 894-902.

Nelson, D.L., Cox, M.M. *Lehninger Principles of Biochemistry*, 3rd ed.; Worth Publishers: New York, 2000.

Ottemann, K., Thorgeirsson, T.E., Kolodziej, A.F., Shin, Y.-K., Koshland, D.E. (1998). Direct measurement of small ligand-induced conformational changes in the aspartate chemoreceptor using EPR. *Biochemistry* **37**, 7062-1069.

Tirado-Rives, J., Maxwell, D.S., Jorgensen, W. (1993). Molecular dynamics and Monte Carlo simulations favor the *alpha*-helical form for alanine-based peptides in water. *J. Am. Chem. Soc.* **115**, 11590-11593.

Zhang, L., Hermans, J. (1994). 3_{10} helix versus α-helix: A molecular dynamics study of conformational preferences of aib and alanine. *J. Am. Chem. Soc.* **116**, 11915-11921.

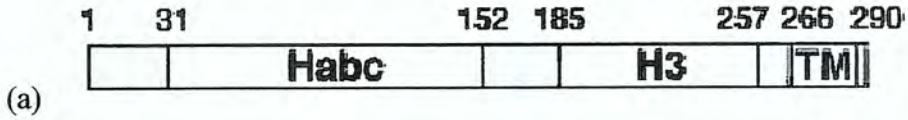

(a)

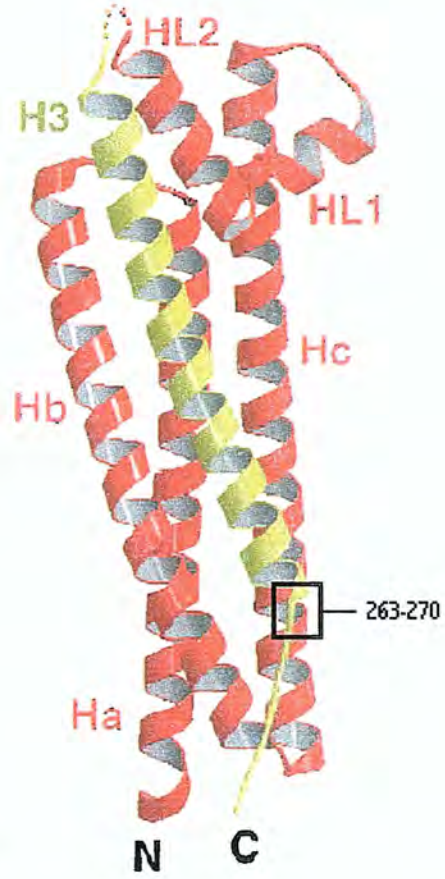

(b)

Figure 3.1. (a) The primary structure for Sso1p. (b) Model of the Sso1p protein. The yellow helix represents the H3 domain of the protein. The straight "stick" in the lower part of the yellow structure is the transmembrane (TM) domain. The spin labeled cysteine mutants are at positions 263 and 270, which is the linker region (adapted from Munson *et al.*, 2000).

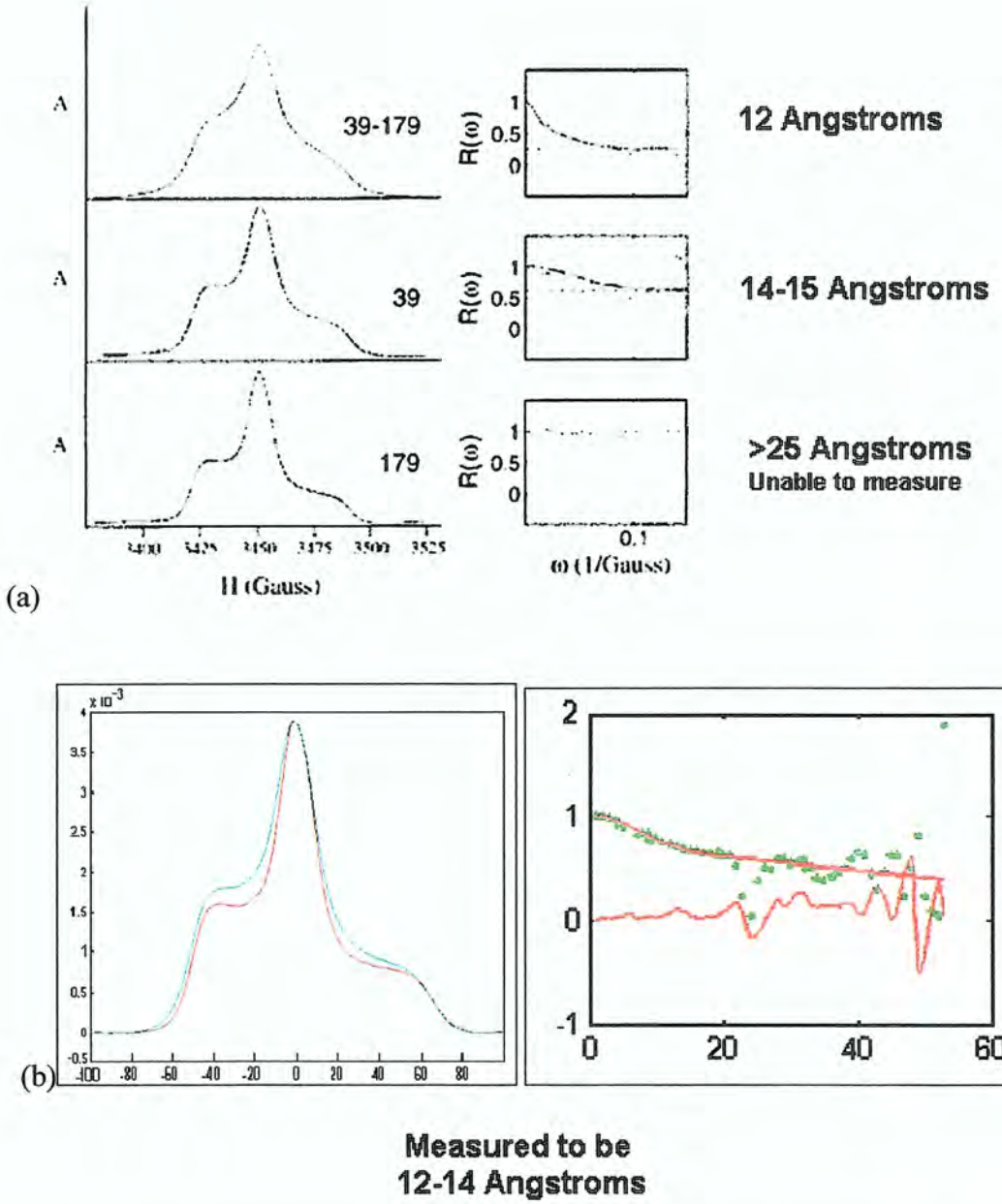

Figure 3.2. (a) Examples of distances measured by the Fourier Deconvolution method (adapted from Ottemann *et al.*, 1998). (b) On the left, the absorbance spectra of spin labeled Sso1p K263C (red), S(B), overlapping with the absorbance spectra of doubly spin labeled Sso1p K263C/V270C, aΠ(B) + bS(B) (blue). The peaks of the center hyperfine lines have been fit, scaled along the y-axis. The data fits well to the sum of two Gaussian functions, as shown in the figure to the right.

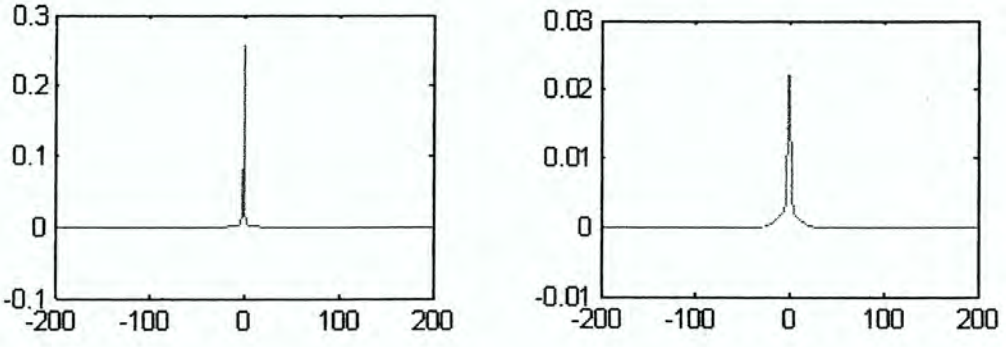

Figure 3.3. Left: the delta function from the y-axis offset in M*(ω). Right: the dipolar function (M(B)) after subtracting the reference spectra.

CHAPTER 4: GENERAL CONCLUSIONS

Conclusions

EPR spectroscopy is a useful tool for determining the structures and mechanisms of biochemical phenomena. Direct distance measurement between spin labeled sites is a useful method of determining the secondary and tertiary structure of proteins and nucleic acids (Hustedt & Beth, 1999; Biswas *et al.*, 2001). The two different types of EPR are a continuous wave or pulses of microwave energy used to excite the spin states of the unpaired electrons of a sample. Both types of EPR have their disadvantages. Continuous wave EPR is useful for measuring small distances (<25 Angstroms) between two spin labeled sites, whereas pulse EPR methods are useful for measuring larger distances beyond 50 Angstroms (Persson *et al.*, 2001)

The Fourier deconvolution method was unable to measure a 32 Angstrom distance at -40°C. However, data analysis suggests the inability to measure the long distance may be a result of different secondary structures of the spin labeled proteins in the reference and interacting spectrums. Presently, the Fourier deconvolution method is capable of measuring up to 25 Angstroms and is the only cwEPR method capable of measuring such a large distance (Rabenstein & Shin, 1995).

SNARE proteins bridge the vesicle membrane with the plasma membrane, and their complex formation is a necessary step for membrane fusion. The fusion of two opposing membranes requires a large amount of energy. It has been suggested the coupling of the core SNARE complex to the membrane harnesses the energy necessary for fusion of the synaptic vesicle with the plasma membrane of a neuron (Kim *et al.*, 2002; Kweon *et al.*, 2002; Kweon

et al., 2003). On the other hand, when the Snc2 post-golgi body v-SNARE forms the core complex, it inserts a helical linker region into the membrane to play more of a set-up role rather than an energetic role for membrane fusion (Chen *et al.*, 2004; Zhang *et al.*, 2005).

Knowledge of the linker region between the SNARE complex and the membrane provides greater insight about the mechanisms necessary for membrane fusion. The linker conformation of the post-golgi body t-SNARE Sso1p was determined based on the distance between residues 263 and 270. When the Sso1p protein is reconstituted into the membrane, the linker region is most likely helical in structure based upon the measured distance of 12–14 Angstroms between residues K263 and V270. This distance measurement supports the immersion depth data from EPR collisional method experiments performed by Yinghui Zhang, a colleague in the Shin laboratory (unpublished data). Zhang's collisional method experiments also suggest that residues 263-265 may be unstructured.

Sso1p is the transmembrane t-SNARE in post-golgi bodi membrane fusion. Its analog neuronal t-SNARE, Syntaxin 1a, also showed an unstructured linker area of approximately 3 residues (Kim *et al.*, 2002; Kweon *et al.*, 2002). This unstructured area may be conserved among transmembrane t-SNAREs. However, further knowledge of other t-SNAREs would be necessary before any general conclusions could be made.

References

Biswas, R., Kuhne, H., Brudvig, G.W., Gopalan, V. (2001). Use of EPR spectroscopy to study macromolecular structure and function. *Science Progress* **84**(1), 45-68.

Chen, Y., Xu, Y., Zhang, F., Shin, Y.-K. (2004). Constitutive versus regulated SNARE assembly: A structural basis. *EMBO* **23**(4), 681-689.

Hustedt, E.J., Beth, A.H. (1999). Nitroxide spin-spin interactions: Applications to protein structure and dynamics. *Annu. Rev. Biophys. Biomol. Struct.* **28**,129-53.

Kim, C.S, Kweon, D.-H., Shin, Y.-K. (2002). Membrane topologies of neuronal SNARE folding intermediates. *Biochemistry* **41**, 10928-10933.

Kweon, D.-H., Kim, C.S., Shin, Y.-K. (2002). The membrane dipped-neuronal SNARE complex: A site-directed spin labeling electron paramagnetic resonance study. *Biochemistry* **41**, 9264-9268.

Kweon, D.-H., Kim, C.S., Shin, Y.-K. (2003). Insertion of the membrane-proximal region of the neuronal SNARE coiled coil into the membrane. *J. Biol. Chem.* **278**(15), 12367-12373.

Perrson, M. Harbridge, J.R., Hammarstrom, P., Mitri, R., Martensson, L.-G., Carlsson, U., Eaton, G.R., Eaton, S.S. (2001). Comparison of electron paramagnetic resonance methods to determine distances between spin labels on human carbonic anhydrase II. *Biophysical* **80**, 2886-2897.

Rabenstein, M.D., Shin, Y.K. (1995). Determination of the distance between two spin labels attached to a macromolecule. *Proc. Natl. Acad. Sci. U.S.A.* **92**, 8239-8243.

Zhang, Y., Su, Z., Zhang, F., Shin, Y.-K. (2005). A partially zipped SNARE complex stabilized by the Membrane. *J. Biol. Chem.* **280**, 15595-15600.

ACKNOWLEDGEMENTS

There are so many people to thank. Most of all, my thanks goes to Rob Hecker, Chang Sup Kim, and Fan Zhang. Rob was always open to discussing the research and numerous papers with me. I could not have completed this research without the instruction and guidance of Xiaolan Yao, Zengliu Su, Chang Sup Kim, and Fan Zhang. I am greatly in their debt. Klaus Schmidt-Rohr and Qiang "Charles" Chen were extremely helpful with the MatLab data programming and analysis of the spectra for the doubly labeled SNAP-25[C].

I also owe a great deal of thanks to my committee members Klaus Schmidt-Rohr and Thomas Greenbowe for their feedback and help to complete my degree requirements.